Available online at www.sciencedirect.com
ScienceDirect
Lithos 92 (2006) 55–82
LITHOS
www.elsevier.com/locate/lithos

CO_2 metasomatism in a basalt-hosted petroleum reservoir, Nuussuaq, West Greenland

Karyn L. Rogers [a,*], Philip S. Neuhoff [b], Asger K. Pedersen [c], Dennis K. Bird [d]

[a] Department of Earth and Planetary Sciences, Washington University, St. Louis, MO 63130, United States
[b] Department of Geological Sciences, University of Florida, Gainesville, FL 32611-2120, United States
[c] Geological Museum, Øster Voldgade 5-7, DK-1350 Copenhagen K, Denmark
[d] Department of Geological and Environmental Sciences, Stanford University, Stanford, CA 94305, United States

Received 11 May 2005; accepted 27 March 2006
Available online 30 June 2006

Abstract

Extensive subaerial exposures of a basalt-hosted petroleum reservoir around Marraat Killiit on Nuussuaq, West Greenland, provide an unparalleled opportunity to investigate water–rock–hydrocarbon interactions in an unconventional petroleum system. Exposed sections in this locality include picritic and olivine-phyric basalts, with both subaerial and subaqueous textures that initially had significant primary porosity in the form of gas vesicles, scorias, and interclast voids within hyaloclastites. Alteration of these low-silica, high-magnesium basalts formed regionally-extensive, silica-deficient zeolite-facies mineral assemblages that dominantly consist of mixed-layer chlorite/smectite clays, thomsonite, natrolite, gonnardite, analcime and chabazite. In the study area, faulting and fracturing allowed petroleum migration from sediments into the overlying basalts. Migration of petroleum and the associated brine led to the pseudomorphic replacement of zeolite and clay mineral assemblages by carbonates (siderite, magnesite, dolomite and calcite) and quartz. Carbonates associated with petroleum migration are rich in Mg and Fe, reflecting the interaction of a CO_2-rich fluid with a picritic basalt and associated Fe- and Mg-rich smectites. Only late stage carbonates are calcium-rich, the result of depletion of aqueous magnesium and iron following precipitation of magnesite–siderite solid solutions. Values of $\delta^{13}C_{vPDB}$ and $\delta^{18}O_{vSMOW}$ of carbonates at Marraat form two distinct groups: (1) paragenetically early dolomite veins and magnesite–siderite replacement of low-grade metamorphic minerals that have $\delta^{18}O_{vSMOW}$ between 12.6 and 20‰ and $\delta^{13}C_{vPDB}$ in the approximate range of 0±5‰, and (2) late stage calcite veins that are lighter in ^{18}O ($\delta^{18}O_{vSMOW}$ between 6.4 and 8.7‰) and have a restricted range of $\delta^{13}C_{vPDB}$ that is near zero. Comparison with isotopic properties of carbonates from petroleum reservoirs worldwide and carbonates formed from meteoric water in basalts from the North Atlantic Igneous Province suggests that the first group of carbonates are formed by reaction of oil field brines with basalts, but the latter group formed by reactions involving meteoric waters.

Reservoir properties and quality are a sensitive function of the sequence of hydrothermal and deformation events affecting this region. Regional metamorphism resulted in extensive occlusion of primary porosity by mafic phyllosilicates and zeolites. Subsequent brittle deformation resulted in the formation of fracture sets that served as migration pathways for hydrocarbons and carbonate-rich brines. Interaction of these brines with the zeolite facies metabasalts resulted in extensive alteration reactions that replaced metamorphic mineral assemblages with carbonate+quartz, and generated significant secondary porosity that hosted the altering fluids and live hydrocarbons. Mineral paragenesis at Marraat

* Corresponding author. Tel.: +1 314 935 5668; fax: +1 314 935 7361.
E-mail address: rogers@levee.wustl.edu (K.L. Rogers).

0024-4937/$ - see front matter
doi:10.1016/j.lithos.2006.04.002

indicates that zeolite and clay stability is a sensitive function of the oxidation state of the system and that this is controlled by water–hydrocarbon–basalt interactions.

Keywords: Basalts; Carbonates; Zeolite facies metamorphism; CO_2 metasomatism; CO_2 sequestration; West Greenland

1. Introduction

Basalt-hosted petroleum reservoirs are increasingly the focus of exploration activities in India (Pendkar and Kumar, 1999), Greenland (e.g., Christiansen, 1994), Japan (Hoshi, 1988) and other locations where thick volcanic sequences overly petroleum source rocks. Petroleum generated from adjacent sedimentary source rocks migrates into basalts under favorable flow conditions. The migration of petroleum into basaltic lavas, as well as the successful recovery of petroleum in basalt-hosted reservoirs, is a sensitive function of porosity and permeability. Primary porosity and permeability are typically high in lavas (porosity up to 50%; permeability from 10^{-9} to 10^{-5} darcy; Freeze and Cherry, 1979). However, secondary minerals such as zeolites and mafic phyllosilicates that have large molar volumes often occlude much of the primary porosity (Manning and Bird, 1991; Neuhoff et al., 1999). Petroleum reservoir quality in basalts is thus a strong function of mineral paragenesis, with reactions between altered basaltic lavas and oil-field waters significantly effecting production potential.

Migration of petroleum and associated aqueous fluids can dramatically change chemical potentials within basaltic lavas, destabilize low-grade metamorphic mineral assemblages, and effect hydrologic properties of the system. For example, addition of reduced carbon from petroleum can lower the oxidation state of the aqueous phase and destabilize preexisting secondary mineral assemblages. This is particularly true for Fe-bearing species, which are dominantly Fe(III) due to the oxidized nature of meteoric fluids involved in the weathering and low-grade metamorphism of the lavas (e.g., Neuhoff et al., 1999; Stefansson and Gislason, 2001; Arnórsson et al., 2002). In some cases, reduced oxidation states controlled by the presence of organic matter may stabilize Ca-bearing minerals relative to carbonate-bearing assemblages, as suggested by the association of prehnite and pumpellyite with pyrobitumen in the Builth Volcanic Group, Wales (Metcalf et al., 1992). Aqueous fluids associated with petroleum are often enriched in both CO_2 and organic acids (e.g., Lundegard, 1985; Kharaka et al., 1993a,b), which attain metastable redox equilibrium (Shock, 1988; Helgeson et al., 1993) and can destabilize secondary mineral assemblages. Many divalent cation-bearing secondary silicates formed during low-grade metamorphism of basaltic lavas are metastable with respect to carbonate-bearing assemblages at elevated CO_2 levels (e.g., Crossey et al., 1984). Thus reactions between petroleum-bearing formation waters and pre-existing mineral assemblages often lead to significant decreases in mineral volume and may generate the secondary porosity necessary for petroleum infiltration and migration (e.g., Surdam et al., 1984; Neuhoff and Bird, 1994; Neuhoff et al., 2000).

The present contribution investigates water–basalt–hydrocarbon interactions through field and petrologic evaluation of CO_2 metasomatism that accompanied development of a basalt-hosted petroleum reservoir in the Marraat area of West Greenland (Fig. 1). Extensive glacial denudation of the flood basalt stratigraphy hosting this reservoir provides some of the best-known subaerial exposures of a basaltic petroleum reservoir. This region is ideal for characterizing the evolution of these systems because exposures allow comparison of adjacent portions of the system that variably experienced the effects of CO_2 metasomatism associated with petroleum migration. Observations of mineral parageneses associated with petroleum infiltration allow temporal and spatial correlation between secondary mineral assemblages and petroleum migration. Field mapping, petrographic analyses, chemical and isotopic analyses, and geochemical models are used to determine the effect of water–basalt–hydrocarbon interactions on secondary mineral stability and fluid flow properties. These observations are used to constrain thermodynamic models of mineral stability, porosity evolution and oxidation state during petroleum and brine migration.

2. Geologic background

The Nuussuaq Basin of West Greenland extends from Disko to Svartenhuk and contains the most extensive outcrops of Mesozoic to Paleogene rocks from the Labrador Sea to Baffin Bay region. The Nuussuaq Basin belongs to a complex of sedimentary basins that are Early Cretaceous or older (Chalmers et al., 1999; Chalmers and Pulvertaft, 2001). The Nuussuaq Basin consists of clastic sediments and volcanic rocks and is underlain by Precambrian gneiss, which is exposed as a tilted horst block extending from south to central Disko. An

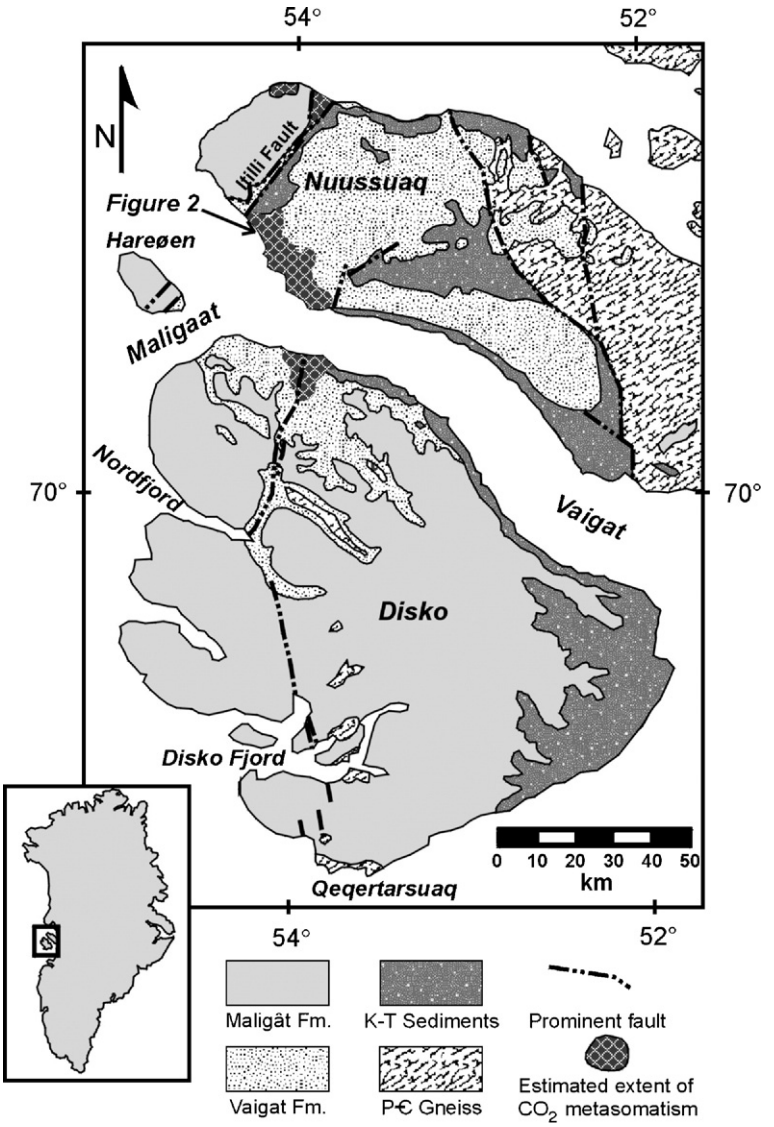

Fig. 1. Generalized geologic map of the Nuussuaq-Disko region in West Greenland. The crosshatched areas indicate outcrops of carbonate altered basalts.

extensional fault system establishes the eastern boundary (Chalmers et al., 1999). In the early to late Cretaceous the basin was filled with approximately 6 km of deltaic deposits including fluvial sandstones, mudstones and coal (Pedersen and Pulvertaft, 1992). In the early Paleocene, three phases of tectonism affected relative sea level and resulted in valley incision and subsequent infilling (Dam, 2002). Late Cretaceous to early Paleocene sediments include turbidite sandstones and shelf mudstones (Dam and Sonderholm, 1994). Flood basalt volcanism commenced around 61 Ma, and the bulk of the lavas (~80%) were erupted within ~1 Ma (Storey et al., 1998). The basalts are exposed from Disko Island in the south (Fig. 1) to Svartenhuk Halvo in the north, covering an area of ~45,000 km^2 with stratigraphic thickness between 2 and ~5 km. The earliest volcanic rocks, which are mostly picrites and magnesian basalts, make up the Vaigat Formation, which contains both subaerial lava flows and subaqueous hyaloclastite breccias (Hald and Pedersen, 1975). The Vaigat Formation is overlain by the Maligât Formation, which is composed of feldspar-phyric tholeiites. Both formations exhibit subaqueous and subaerial textures, indicating extensive basin movements and volcanic infilling in large marine basins (Clarke and Pedersen, 1976; Henderson et al., 1981; Pedersen, 1985; Pedersen et al., 2002). Following a ca. 6 m.y. hiatus, less voluminous volcanism resumed in the earliest Eocene and continued through at least 52.5 Ma with sporadic intrusive

events until about 27 Ma (Storey et al., 1998). Flood basalts throughout the region experienced varying degrees of zeolite to prehnite–actinolite facies metamorphism in response to burial and hydrothermal alteration around dikes and faults (Christiansen et al., 1999; Neuhoff et al., 2006-this issue).

The present study focuses on the Marraat area of the Nuussuaq peninsula (Fig. 2) where the lowest member of the Vaigat Formation, the Anaannaa Member, is exposed (Pedersen et al., 2002). The Anaannaa Member consists of picrites and olivine-phyric basalts overlain by more evolved aphyric and feldspar-phyric basalts. The entire Anaannaa Member exhibits lateral facies transitions between subaqueous and subaerial textures, which are juxtaposed throughout Marraat by post-depositional faults associated with compression along the Itilli Fault Zone to the west (Figs. 1 and 2). There is also evidence of significant diking prior to petroleum migration at Marraat, with nearly 10% dike density in some areas (Christiansen et al., 1996).

Evidence of hydrocarbons in the Nuussuaq area was first reported as gas recovery in 1969 (Henderson, 1969) and later corroborated by reports of solid bitumen found in the basalts (Pedersen, 1986). However, evidence of a significant source of oil in the region was not discovered until 1992 (Christiansen, 1993). Bitumen staining of the basalts is common at Marraat and liquid petroleum fills vugs and pores in the lava flows (Fig. 3). Subsequent field and analytical studies led to the discovery of five different types of petroleum source rocks in the basalts at Marraat and suggested that there was active replenishment of petroleum into the basalts from the underlying source rocks (Christiansen et al., 1994, 1996; Bojesen-Koefoed et al., 1999). While drilling at Marraat has not penetrated the source rocks for the hydrocarbons, the petroleum types identified at Marraat are consistent with a deltaic depositional environment (Bojesen-Koefoed et al., 1999). This suggests that at least some of the source rocks generating the petroleum found at Marraat are related to the Late Cretaceous to early Paleogene deltaic sediments that crop out in the Itilli Valley, on the south coast of Nuussuaq, and on the northern and eastern coasts of Disko (Fig. 1). Northwest–southeast striking faults that cut the basalts (Fig. 2), and presumably the underlying sediments, at Marraat have been hypothesized as conduits for

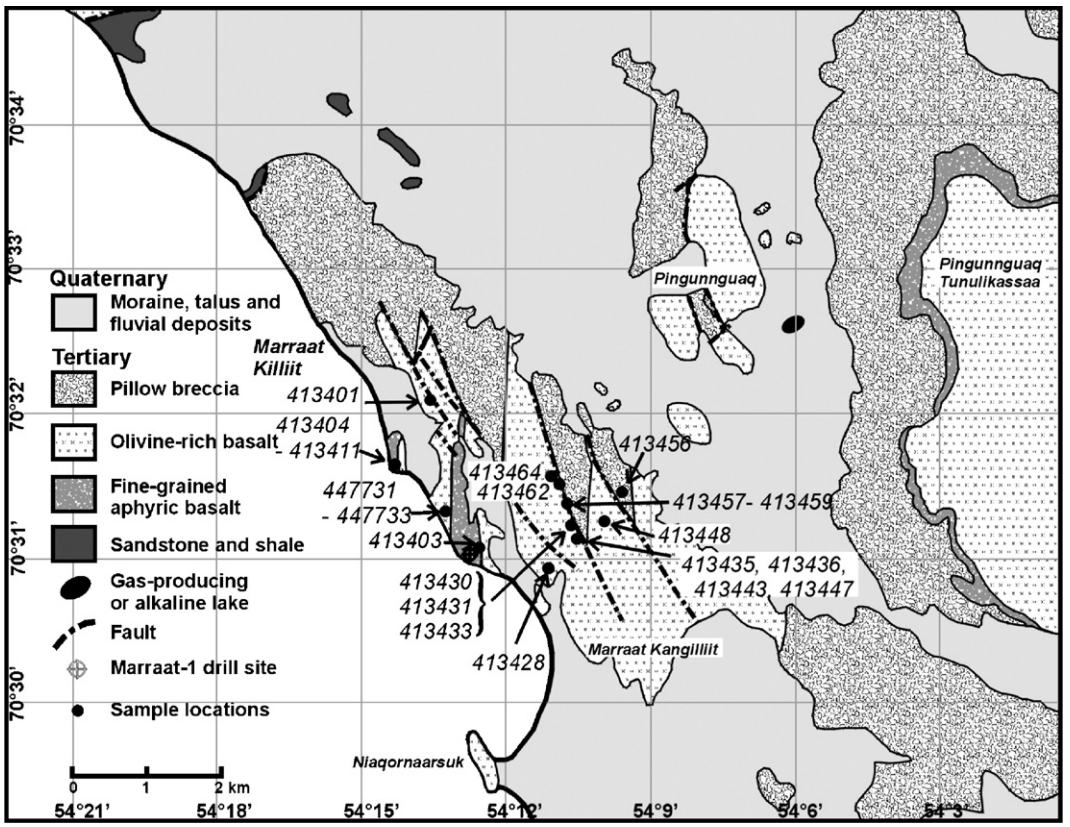

Fig. 2. Map of the Marraat area modified from Christiansen et al. (1994) and Henderson (1975), enlargement of the area shown in Fig. 1. Sample numbers indicate those used in the present study and in Rogers (2000).

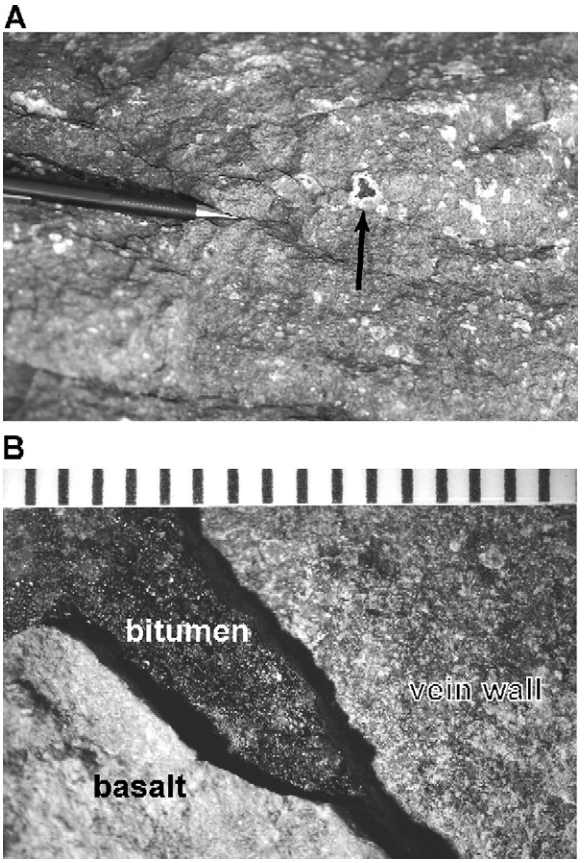

Fig. 3. Hydrocarbon occurrences at Marraat. (A) Tarry bitumen inside a carbonate-lined vesicle (see arrow); pencil for scale. (B) Tarry bitumen lining center of vein in sample 447733; ruler marks in mm. View is looking at the plane of the vein; the black bitumen is exposed where the top portion of the vein has been removed.

petroleum from the underlying Cretaceous sediments to migrate into the overlying basalts (Christiansen et al., 1999). Similar styles of petroleum occurrence have been observed through a large part of the basin, including the south coast of Svartenhuk peninsula, Ubekendt Ejland, Harøen, and the northern coast of Disko island (Fig. 1; Pedersen, 1986; Christiansen et al., 1996; Bojesen-Koefoed et al., 1997a,b; Christiansen et al., 1998).

3. Methods

Outcrop mapping and sampling of secondary alteration minerals at the Marraat area was conducted during the summer of 1997 as part of an expedition by the Geological Survey of Denmark and Greenland (GEUS). Mapping included detailed observations of secondary mineral parageneses, structural orientations, and timing relationships. Several hundred samples representative of low-grade metamorphic and carbonate altered basalts were collected in conjunction with these observations. Of these samples, 24 were chosen as representative of both regional zeolite and local carbonate alteration (Fig. 2).

Mineral parageneses in the samples were assessed using a combination of petrographic, electron microprobe, and X-ray diffraction techniques. Compositions of primary and secondary minerals were determined by electron microprobe analysis on a JEOL 773A electron microprobe operated at 15 kV with a 15 nA beam current. Calibrations were based on natural geologic standards. Beam width was increased to 10–20 μm for clays, zeolites and carbonates (when grain size allowed) in order to reduce volatile and alkali loss. Values presented below are averages of triplicate analyses. In cases where mineral composition varied within a grain as a function of morphology, single-point analyses were conducted at 10–30 locations along a traverse through the grain. The data were first corrected for oxygen present in molecular and structural water sites in hydrous minerals and then converted to oxide weight percents using the CITZAF correction procedure (Tingle et al., 1996). Mineral separates were characterized with X-ray powder diffraction (XRPD) using a Rigaku theta–theta diffractometer with Cu*K*α radiation operating at 35 kV and 15 mA.

Eighteen carbonates representative of the different textures and parageneses described below from eight different hand samples were separated using a micro-drill for carbon and oxygen isotope analysis. Carbonate powders were analyzed at the Paul H. Nelson Stable Isotope Laboratory at The University of Iowa. All powdered samples were vacuum-roasted at 380 °C to remove volatile contaminants. Individual samples were then reacted with anhydrous phosphoric acid at 72 °C using a Kiel III automated single sample carbonate reaction device coupled to the inlet of a Finnigan MAT 252 isotope ratio mass spectrometer (analytical precision of better than ±0.05‰). For comparative analysis we evaluated carbon and oxygen isotopes in calcites from altered Tertiary basalts of Ubekendt Island, West Greenland, basalts near the Skaergaard intrusion in East Greenland, and from Eastern Iceland at both the Paul H. Nelson Stable Isotope Laboratory at The University of Iowa and the Stable Isotope Biogeochemistry Laboratory at Stanford University. Procedures at the Stable Isotope Biogeochemistry Laboratory are as follows. Powdered samples (150 to 300 μg) of carbonate were reacted at 70 °C with anhydrous phosphoric acid in sealed reaction vessels flushed with helium gas. Headspace sampling of evolved CO_2 was performed with a Finnigan Gas-Precision Bench, and isotopic ratios measured on a Finnigan Delta+XL mass spectrometer (precision of carbonate isotopic data is ~0.2‰ for both oxygen and carbon

isotope ratios based on repeated analyses of NBS-18 and NBS-19 carbonate standards). All isotopic values are reported relative to the vPDB standard for both carbon and oxygen. Values of $\delta^{18}O$ were converted to the SMOW standard using the correction given by Hoefs (1987).

4. Results

4.1. Field relations

Detailed mapping in the Marraat area (Fig. 2) illustrates a complex history of regional low-grade metamorphism, faulting, dike emplacement, hydrocarbon migration, and hydrothermal alteration associated with CO_2 metasomatism. Fig. 4 summarizes the relative timing of basalt alteration associated with low-grade metamorphism and of later vein mineral assemblages. Field relations among the mineral parageneses depicted in Fig. 4 are summarized below.

The earliest alteration observed is the partial or complete infilling of primary porosity (e.g., vesicles, scoriaceous and brecciated lava flow tops, intraclast pore space in hyaloclastites) by silica and silicate mineral assemblages formed during regional low-grade metamorphism of basalts. Mafic phyllosilicates, zeolites, quartz, and recrystallized opal are the most abundant secondary minerals. The low-grade metamorphic mineral assemblages are part of a regionally distributed sequence of depth-controlled zeolite zones occurring throughout the flood basalt province (Christiansen et al., 1999; Neuhoff et al., 2006-this issue). In the Marraat area, the low-grade metamorphic assemblages are overprinted by later assemblages of carbonates and silica minerals associated with the development of prominent faults and veins, and the migration of petroleum.

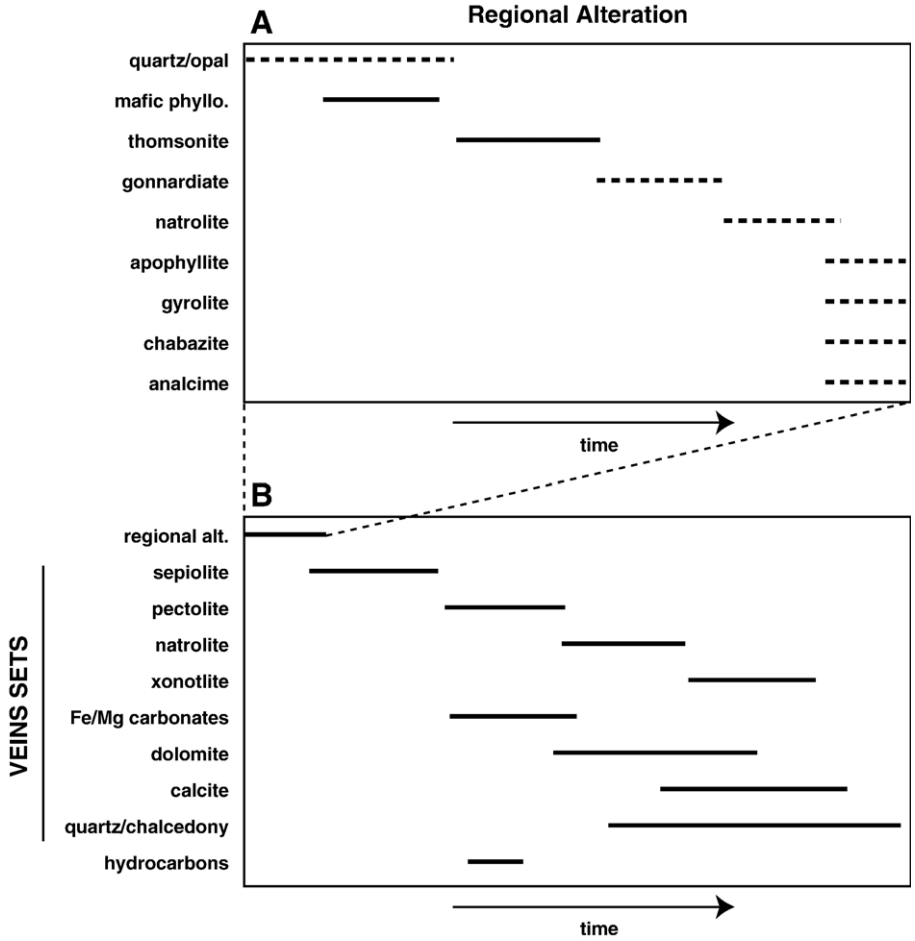

Fig. 4. Relative timing of mineral paragenesis in basalts from the Marraat area during (A) regional low-grade metamorphism and during (B) fracture filling events (veins). Dashed horizontal lines in (A) indicate phases that are observed in some but not all samples. Abbreviations: Phyllo = phyllosilicates; Alt = alteration.

Numerous vein sets are present within the basalts. The most common veins contain Ca-rich carbonate minerals (dolomite or calcite) and quartz, although localized swarms of veins filled with sepiolite, natrolite, xonotlite, or pectolite are present (Karup-Møller, 1969; Binzer and Karup-Moller, 1974). In most cases, these vein sets crosscut pores filled with regional metamorphic minerals, and it is inferred that veining was developed subsequent to regional metamorphism. Sepiolite veins are the earliest, and are crosscut by all other vein types. Although Karup-Møller (1969) suggested that the distribution of pectolite, natrolite, and xonotlite veins are stratigraphically controlled, we have observed all vein types within single outcrops. Furthermore, the xonotlite veins crosscut mafic dikes. The relative timing of carbonate veins (including those containing hydrocarbons) is ambiguous, and it appears from crosscutting relationships that several generations of these veins are present in the region. Within one (or more) of the earlier carbonate vein sets hydrocarbons occur as tarry residues in the centers of veins, as stains on carbonate crystals, or as fluid inclusions within the carbonates. Clear evidence of alteration of the surrounding basalts by the fluids associated with silicate-filled veins is limited. In contrast, there is extensive metasomatic alteration of basalts associated with the carbonate veins.

4.2. Regional low-grade metamorphism

The earliest alteration of basalts involves formation of mafic phyllosilicates, zeolites, and silica minerals formed during regional low-grade metamorphism. Detailed descriptions and interpretation of these parageneses are given in a companion paper in this volume (Neuhoff et al., 2006-this issue), and are summarized below. Amorphous silica is the first to form, precipitated as pore space linings in vesicles and in brecciated lava flow tops. Texturally superposed on amorphous silica are pore space linings of mafic phyllosilicates consisting of mixed layer chlorite–smectite and mixed dioctahedral–trioctahedral smectites. Within open pore space mafic phyllosilicates are overgrown by one or more zeolite minerals. In the basalt matrix primary olivine, glass, and pyroxene are variably replaced by these secondary phases. Paragenetic relationships among silica minerals, chlorite/smectite and the various zeolite species are summarized in Fig. 4.

Table 1
Representative compositions of mafic phyllosilicates in basalts from Marraat, West Greenland

Sample	413403-10	413462-1	413430-2	413401-4	413403-8
Oxide weight percent					
SiO_2	54.07	41.13	43.33	36.85	47.50
TiO_2	0.15	1.70	0.02	0.02	0.06
Al_2O_3	11.49	9.42	8.54	9.72	8.25
FeO[a]	11.65	15.94	12.19	12.21	16.08
MnO	0.01	0.22	0.18	0.13	0.05
MgO	7.50	15.60	18.89	27.13	11.56
CaO	1.67	4.04	2.97	0.42	2.00
Na_2O	0.26	0.15	0.16	0.07	0.26
K_2O	0.34	0.03	0.10	0.05	0.19
BaO	0.03	0.01	0.00	0.00	0.03
Total	87.16	88.24	86.39	86.59	85.97
Anhydrous formula unit composition					
Si	9.97	8.14	8.44	7.25	9.30
Ti	0.03	0.25	0.00	0.00	0.00
Al	2.50	2.20	1.95	2.25	1.90
Fe	1.81	2.64	1.99	2.01	2.66
Mn	0.00	0.04	0.04	0.03	0.00
Mg	2.06	4.61	5.48	7.96	3.41
Ca	0.33	0.86	0.61	0.09	0.41
Na	0.10	0.07	0.07	0.04	0.09
K	0.08	0.00	0.04	0.00	0.04
Ba	0.00	0.00	0.00	0.00	0.00
O[b]	28	28	28	28	28

Sample descriptions: Sample 413403 is a vesicular picrite with traces of hydrocarbon. Sample 413462 is a brecciated picrite cut by a vein filled with sparry calcite and oil. Samples 413430 and 413401contain thomsonite and mafic phyllosilicates filling the vesicles.

[a] Total Fe reported as FeO.

[b] Oxygen charge equivalents per formula unit.

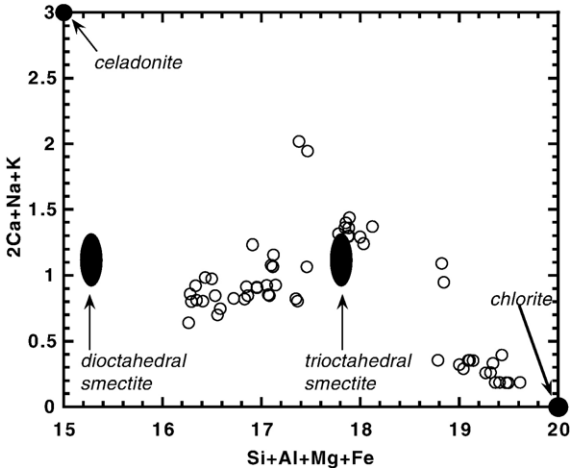

Fig. 5. Composition of mafic phyllosilicates in basalts from the Marraat area, normalized to 28 oxygen charge equivalents. The total moles of charge of exchangeable cations (2Ca+Na+K) are plotted as a function of the total molar (Si+Al+Mg+Fe) content. Ideal end member compositions of chlorite, celadonite, trioctahedral smectite and dioctahedral smectite are depicted as filled ovals and circles.

Mafic phyllosilicates typically occur as several generations of thin greenish-brown linings of pore spaces and as extensive pseudomorphs of olivine and mesostasis within the matrix of the lavas. Representative analyses of mafic phyllosilicates from Marraat are given in Table 1. Mafic phyllosilicate compositions are consistent with observations from other parts of the province (Neuhoff et al., 2006-this issue) and comprise two distinct compositional trends corresponding to mixtures of *i)* trioctahedral smectite and chlorite and *ii)* dioctahedral smectite and trioctahedral smectite as illustrated in Fig. 5. Because of the fine scale of layering between mafic phyllosilicates and intra-sample heterogeneity, no attempt was made to determine the nature of the interlayerings. However, in similar samples with nearly identical phyllosilicate compositions from County Antrim, Ireland, Robert (2001) found evidence for both discrete chlorite and randomly interstratified chlorite–smectite. The typical texture of these phases is illustrated in Fig. 6C, in which a thin layer of mixed dioctahedral–trioctahedral smectite lines the pore (followed by a rim of silica).

Most of the primary porosity in the basalts was filled during regional low-grade metamorphism by zeolites. The most common zeolites at Marraat are fibrous bundles of thomsonite, gonnardite, and natrolite; however, chabazite and analcime are also observed late in the paragenesis (Fig. 4). Thomsonite is frequently the earliest

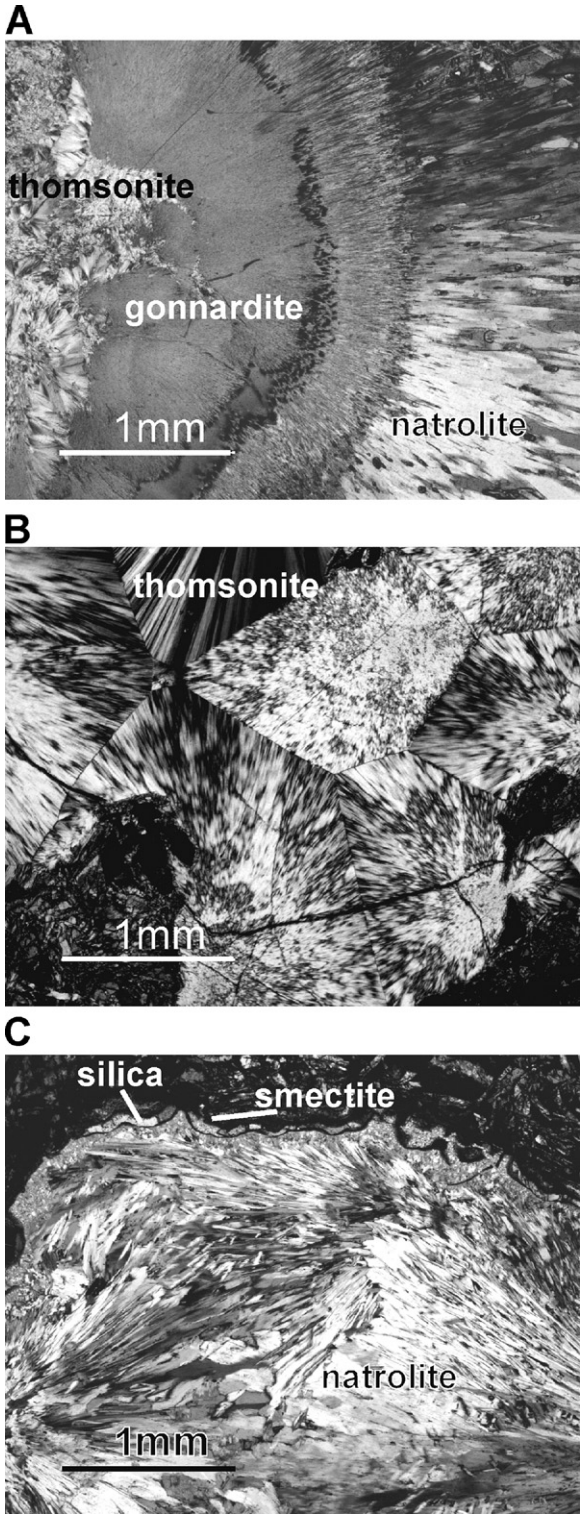

Fig. 6. Regional metamorphic mineral assemblages at Marraat. (A) Sample 413433 thin section of vein (nicols partially crossed) showing the dominant paragenesis of early thomsonite followed by gonnardite and later natrolite. Note irregular structure defined by the boundary of the gonnardite mass. (B) Sample 413447 showing typical morphology of thomsonite with straight boundaries between the fibrous bundles. (C) Sample 413458 with natrolite-filled pore lined with dioctahedral–trioctahedral smectite and silica.

Table 2
Representative compositions of zeolites in basalts from Marraat, West Greenland

Sample	413436	413436	413436	413436	413436	413462	413430	413436	413436
Zeolite	Thomsonite	Gonnardite	Thomsonite	Gonnardite	Natrolite	Analcime	Chabazite	Gonnardite	Thomsonite
Oxide weight percent									
SiO_2	38.46	45.24	38.29	44.30	44.78	56.63	51.18	43.09	39.18
TiO_2	0.00	0.01	0.02	0.02	0.01	0.00	0.02	0.00	0.01
Al_2O_3	29.01	27.59	29.00	27.64	27.30	21.98	22.71	28.21	29.86
FeO[a]	0.10	0.06	0.08	0.08	0.08	0.15	0.09	0.08	0.07
MnO	0.04	0.06	0.08	0.06	0.04	0.07	0.04	0.07	0.07
MgO	0.00	0.00	0.09	0.00	0.00	0.00	0.00	0.00	0.00
CaO	12.36	1.54	12.21	1.89	0.12	0.02	7.64	3.78	11.78
Na_2O	4.29	14.50	4.23	14.05	15.84	13.36	4.61	12.31	4.54
K_2O	0.00	0.00	0.00	0.00	0.00	0.01	0.43	0.00	0.01
BaO	0.03	0.00	0.00	0.02	0.01	0.02	0.00	0.01	0.00
total	84.29	89.01	84.00	88.05	88.19	92.24	86.72	87.56	85.53
Anhydrous formula unit composition									
Si	5.28	5.84	5.27	5.78	2.92	2.06	3.95	4.68	5.28
Ti	0.00	0.00	0.00	0.00	0.00	0.00	0.00	0.00	0.00
Al	4.69	4.20	4.70	4.26	2.10	0.94	2.07	4.38	4.75
Fe	0.00	0.00	0.00	0.00	0.00	0.01	0.00	0.00	0.00
Mn	0.00	0.00	0.01	0.00	0.00	0.00	0.00	0.00	0.00
Mg	0.00	0.00	0.02	0.00	0.00	0.00	0.00	0.00	0.00
Ca	1.82	0.22	1.81	0.26	0.01	0.00	0.63	0.52	1.71
Na	1.14	3.62	1.13	3.56	2.00	0.94	0.69	3.14	1.19
K	0.00	0.00	0.00	0.00	0.00	0.00	0.04	0.00	0.00
Ba	0.00	0.00	0.00	0.00	0.00	0.00	0.00	0.00	0.00
O[b]	20	20	20	20	10	6	12	20	20

Sample descriptions: Sample 413436 is a vesicular picrite with thomsonite- and gonnardite-filled vesicles and is cut by a natrolite vein. Sample 413462 is a brecciated picrite cut by a vein filled with sparry calcite and oil. Sample 413430 is a vesicular picrite with zeolites and mafic phyllosilicates filling the pore spaces.

[a] Total Fe reported as FeO.

[b] Number of oxygens in anhydrous formula unit.

zeolite to form, followed by gonnardite and then end member natrolite as illustrated in the photomicrograph in Fig. 6A. Fig. 6B illustrates the typical texture of thomsonite pore fillings, with sharp, continuous boundaries between individual crystal bundles. Natrolite most often occurs as individual acicular crystals rather than bundles of crystals as with thomsonite and gonnardite (Fig. 6C). Chabazite and analcime are rare and are always formed after the fibrous zeolites. Locally apophyllite and gyrolite are found as the last phases to form within vesicles.

Representative compositions of zeolites from Marraat are listed in Table 2. Natrolite and analcime compositions are close to their stoichiometric formulas ($Na_2Al_2Si_3O_{10}\cdot nH_2O$ and $NaAlSi_2O_6\cdot nH_2O$, respectively). Chabazite exhibits a Si/Al ratio of ~2.00 and contains variable amounts of Ca and Na. Thomsonite compositions span the entire range for this solid solution ($Ca_2NaAl_5Si_5O_{20}\cdot nH_2O$ to $Ca_{1.5}Na_{1.5}Al_{4.5}Si_{5.5}O_{20}\cdot nH_2O$). Gonnardite compositions are variable but tend to have Si/Al ratios of 1.4 to 1.5 and Ca/Na ratios of ~2.

4.3. Carbonate–silica alteration at Marraat

Carbonate mineralization is widespread in the basalts of the Nuussuaq peninsula, as illustrated by the hatched areas in the map of Fig. 1. At Marraat (Fig. 2) carbonate mineralization occurs in veins, filling primary porosity, and replacing mafic phyllosilicates and zeolites formed earlier within the primary porosity (Fig. 8). Quartz and chalcedony are often associated with carbonate mineralization. Field relations and textural evidence indicate that the formation of carbonate minerals is genetically related to fractures (faults) and associated vein sets. Areas of widespread carbonate replacement of secondary minerals within vesicles and carbonate infilling of primary porosity are restricted to the proximity of carbonate filled veins. In some cases veins are observed intersecting pores filled with similar carbonate parageneses (Fig. 8A). Petroleum is often associated with carbonates, either as a distinct phase within pores or vein centers, or as fluid inclusions within the carbonates (Fig. 3). Field relations are ambiguous as to the number and timing of carbonate

Table 3
Representative compositions of carbonates in basalts from Marraat, West Greenland

Sample	413403	413403	413403	413406	413406	413407	413407	413407
Morphology	Replacement	Replacement	Pore filling	Pore filling	Replacement	Pore filling	Replacement	Replacement
Oxide weight percent								
SiO_2	0.05	0.06	0.00	0.00	0.00	0.00	0.00	0.29
TiO_2	0.01	0.01	0.00	0.00	0.00	0.01	0.00	0.01
Al_2O_3	0.00	0.00	0.00	0.00	0.00	0.00	0.00	0.00
FeO [a]	23.70	24.28	1.57	3.35	6.82	1.37	11.92	3.05
MnO	0.66	0.59	1.18	0.08	0.21	0.04	0.35	0.06
MgO	21.82	21.97	0.90	19.85	40.87	21.83	33.41	44.75
CaO	7.15	7.17	55.35	34.84	0.49	28.41	4.87	0.68
Na_2O	0.04	0.03	0.00	0.00	0.01	0.01	0.01	0.01
K_2O	0.00	0.00	0.00	0.00	0.00	0.00	0.00	0.00
BaO	0.00	0.00	0.01	0.00	0.00	0.01	0.03	0.01
CO_2 [b]	45.68	45.50	42.89	45.77	50.69	47.78	49.44	49.44
Sum	99.11	99.60	102.23	103.89	99.10	99.45	99.35	100.23
Anhydrous formula unit composition								
Mineral	Fe-magnesite	Fe-magnesite	Calcite	Dolomite	Magnesite	Dolomite	Fe-magnesite	Magnesite
Si	0.00	0.00	0.00	0.00	0.00	0.00	0.00	0.00
Ti	0.00	0.00	0.00	0.00	0.00	0.00	0.00	0.00
Al	0.00	0.00	0.00	0.00	0.00	0.00	0.00	0.00
Fe	0.32	0.33	0.02	0.04	0.08	0.02	0.15	0.04
Mn	0.01	0.01	0.02	0.00	0.00	0.00	0.00	0.00
Mg	0.53	0.53	0.02	0.46	0.89	0.50	0.75	0.95
Ca	0.12	0.12	0.98	0.58	0.01	0.47	0.08	0.01
Na	0.00	0.00	0.00	0.00	0.00	0.00	0.00	0.00
K	0.00	0.00	0.00	0.00	0.00	0.00	0.00	0.00
Ba	0.00	0.00	0.00	0.00	0.00	0.00	0.00	0.00
C [b]	1.01	1.00	0.98	0.96	1.01	1.01	1.01	1.00
O [b]	3.00	3.00	3.00	3.00	3.00	3.00	3.00	3.00

Sample descriptions: Sample 413403 is a slightly vesicular picrite containing traces of hydrocarbons. Sample 413406 is an extremely vesicular picrite cut by veins containing calcite, quartz and oil. Sample 413407 is a vesicular picrite cut by a carbonate vein and shows extensive pseudomorphic replacement of pore-filling zeolites.

[a] Total Fe reported as FeO.

[b] calculated based on CO_3 in formula unit.

mineralization events (although they clearly postdate the regional low-grade metamorphism); however, petroleum-bearing carbonate veins are distinctly crosscut by later carbonate vein sets that do not contain evidence of petroleum. Although not all carbonate mineralization is visibly associated with hydrocarbons at the thin section scale, examples are present of hydrocarbons associated with all of the textural and paragenetic stages described below except late stage calcite veins.

Three types of carbonate minerals are found at Marraat: (1) magnesite ($MgCO_3$)–siderite ($FeCO_3$) solid solutions, (2) dolomite [$CaMg(CO_3)_2$] with minor solid solution of ankerite [$FeMg(CO_3)_2$], and (3) near stoichiometric calcite ($CaCO_3$), (Table 3; Fig. 7). In general, the composition of carbonate minerals is closely related to their paragenesis (Fig. 7). Based on textures and paragenetic relationships we can distinguish three dominant carbonate occurrences in the porosity of the basalts: *i*) carbonates replacing preexisting secondary minerals, *ii*) carbonates filling primary pores (usually in close association with the replacement carbonates), and *iii*) carbonates filling or lining fractures (i.e., veins).

Carbonate veins typically contain combinations of massive microcrystalline carbonate infillings, sparry carbonates, and quartz+/− chalcedony. Vein width is variable, ranging from microns to tens of centimeters in thickness. Occasionally veins are sequentially lined with two or more generations of these textures (Fig. 8B). Carbonate compositions within veins are generally either near end member calcite or dolomite with minor ankerite solid solution (Fig. 7), and typically there is little compositional variation within a given vein. In areas with abundant carbonate veins, most of the primary porosity in the basalts is filled with carbonate minerals. Quartz is often associated with these parageneses. The most common textures in vesicles are radial masses of microcrystalline aggregates of

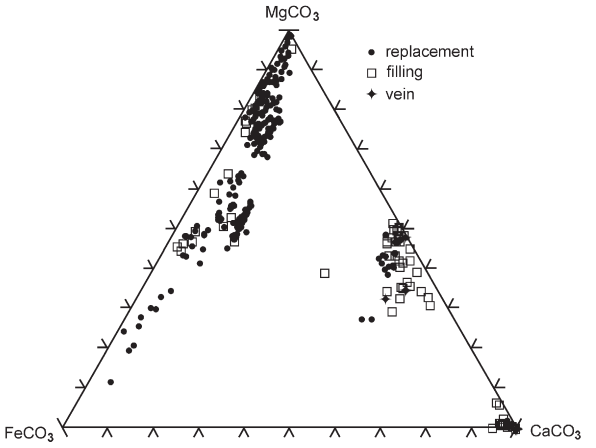

Fig. 7. Ternary diagram showing the compositions of carbonate minerals in basalts at Marraat as a function of paragenetic morphologies including replacement of mafic phyllosilicates and zeolites (solid circles), filling of primary porosity in the basalts (i.e., vesicles and brecciated flow tops; open boxes), and filling of fractures (veins; crosses). Additional data from Rogers (2000).

carbonates +/− quartz that have a bulk morphology identical to mafic phyllosilicates and to radial zeolites (thomsonite and gonnardite) formed during regional metamorphism (see photomicrographs in Fig. 8C through E). Shown in Fig. 8C is a carbonate lining a vesicle that exhibits a semi-radial morphology similar to that typically observed in mafic phyllosilicates in low-grade metabasites. Fig. 8D and E illustrate carbonate textures interpreted to be replacements of thomsonite and gonnardite based on the textural similarity with the zeolite examples shown in Fig. 6A and B. Not only do the carbonates depicted in Fig. 8D and E have a radial habit similar to that of thomsonite and gonnardite, but those in Fig. 8E also exhibit the distinctive sharp, linear boundary between fiber bundles that is typical of thomsonite.

Carbonates forming pseudomorphic replacements of mafic phyllosilicates and zeolites are primarily magnesite–siderite solid solutions, most with compositions of >0.5 mole fraction Mg and little or no Ca (Fig. 7). As illustrated in Fig. 7 there is a near complete range of compositions along the magnesite–siderite solid solution, with Mg mole fractions from ~0.1 to 1 and Fe(II) mole fractions from ~0 to 0.9. The compositions of carbonates within the radial masses are variable, but generally not in a systematic manner. Fig. 9A through C illustrate compositional characteristics of pseudomorphic radial carbonates as a function of distance from the center of the radiating mass to the edge. The samples in Fig. 9A and B are Mg-rich carbonates from vesicles exhibiting minor compositional variation along the magnesite–siderite join. The carbonate analyses shown in Fig. 9C are from a Fe-rich radial mass in a vein that exhibits compositional variations. Fig. 9D shows the nearly uniform composition of dolomite within a vein that crosscuts a radial replacement carbonate.

In some cases, late stage carbonates and quartz are found as sparry vesicle fillings. These infillings appear to be paragenetically late relative to replacement carbonates described above. In all cases, these pore fillings have compositions similar to the dolomites and calcites found in veins (Fig. 7). Examples of these infillings are shown in Fig. 8C and D. Individual crystals from this texture are generally subhedral, but in some instances dogtooth-habit calcite crystals are observed.

4.4. Oxygen and carbon isotopes

Values of $\delta^{13}C_{vPDB}$ and $\delta^{18}O_{vSMOW}$ for eighteen carbonate minerals representative of the various textural and paragenetic types found in Marraat basalts are given in Table 4. Taken as a group, $\delta^{13}C$ of the carbonates range from −5.85 to 5.11‰ PDB and $\delta^{18}O$ ranges from 6.42 to 20.17‰ SMOW. The carbonates were grouped by textural and paragenetic relationships and values of $\delta^{13}C$ are plotted as a function of $\delta^{18}O$ in Fig. 10. The values of $\delta^{13}C$ in the carbonates are not obviously correlated with respect to morphology or paragenetic stage. However, the carbonates associated with petroleum — early vein fillings, replacements and adjacent pore fillings — show a wider range in $\delta^{13}C$ (>10‰) than the late vein fillings that are not associated with petroleum (−1.17 to 0.08‰). Note that values of $\delta^{18}O$ of the carbonates decrease with paragenetic stage. Very early dolomite veins containing bitumen are relatively heavy in ^{18}O ($\delta^{18}O$=19.64 to 19.80‰), as are carbonates associated with replacement of low-grade metamorphic minerals and related infilling of adjacent pores ($\delta^{18}O$=12.60 to 20.17‰), while the very late vein filling calcites are up to 15‰ lighter, with $\delta^{18}O$ values between 6.42 and 8.72‰. Carbonates replacing mafic phyllosilicates are slightly heavier in ^{18}O than zeolite replacements, but there is no consistent trend between replacement carbonates and adjacent pore filling carbonates. All of the carbonates given in Table 4 and Fig. 10 are associated with petroleum migration with the exception of the late calcite veins.

For comparative analysis with the Marraat carbonate mineralization, we have analyzed carbon and oxygen isotopes in thirty-six calcites from a variety of paragenetic origins in Tertiary basalts of West and East Greenland, and from Eastern Iceland. The results are given in Table 5, as well as brief sample descriptions.

It is interesting to note that the range in $\delta^{18}O$ of the calcites (excluding two samples, 4777833ca and Bulandsa) is nearly identical to the range in $\delta^{18}O$ of calcites in the late stage veins at Marraat. However, it is apparent from the data in Table 5 that $\delta^{13}C$ of the calcites includes a wide range of values, from about 2 to

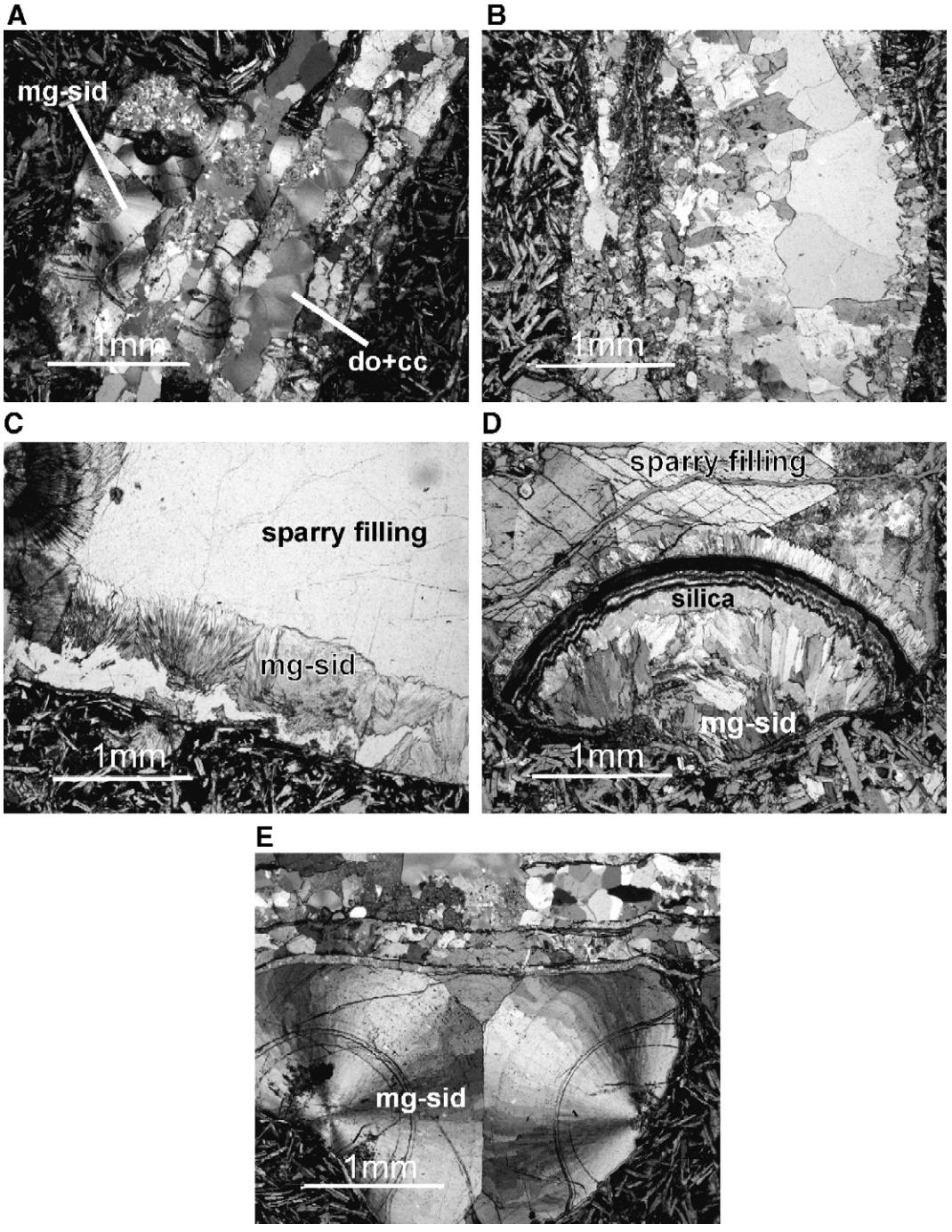

Fig. 8. Carbonate mineralization at Marraat. (A) Pair of dolomite- and calcite-filled (do+cc) veins intersecting a vesicle in which the pre-existing thomsonite has been replaced by magnesite–siderite solid solution (mg–sid; sample 413407). (B) Carbonate vein exhibiting progressive infilling by two generations of calcite (sample 413406). (C). Vesicle in which preexisting mafic phyllosilicates have been replaced by magnesite–siderite solid solution and open space subsequently filled by sparry calcite (sample 413403). (D). Carbonate plus silica replacement of a fibrous zeolite bundle such as that shown in Fig. 6B. Late infilling in the pore is dolomite. (sample 447732). (E) Replacement of thomsonite bundles by magnesite–siderite solid solution (sample 413402).

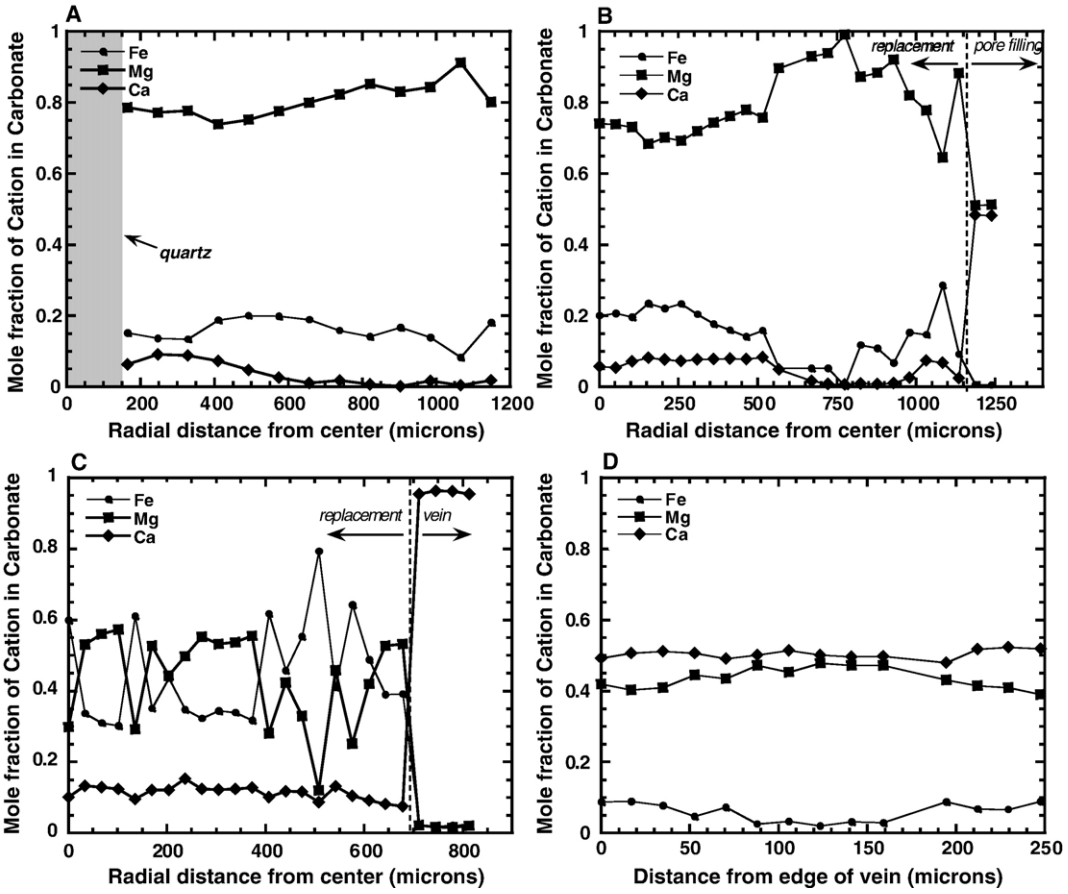

Fig. 9. Spatial variation in composition of replacement, pore filling and vein carbonates in basalts from Marraat. Mole fractions of Ca, Mg and Fe(II) end member carbonates are given as a function of distance from center of radial carbonate pseudomorphs of zeolites or as a function of distance from the edge of a vein. (A) Sample 413408A-1a, magnesite-rich carbonate replacing a radial zeolite, the center of the radial pseudomorph is quartz. (B) Sample 413407-2, magnesite-rich carbonate replacing a radial zeolite (distances 0 to 1150 μm) in contact with pore filling dolomite (distances > 1150 μm). (C) Sample 413403-17, magnesite–siderite solid solution replacing a radial zeolite in a vein subsequently filled with calcite (distances > 700 μm). The vertical dashed lines in B and C indicated the outer edge of the radial zeolite pseudomorphs. (D) Sample 413406-7 vein filling dolomite.

−30 ‰. The data in Table 5 are discussed below with respect to the origin of carbonate minerals at Marraat.

5. Discussion

The complex sequence of tectonic, magmatic, hydrothermal, and fluid transport events recorded in the Marraat area have had a profound effect on the properties of the petroleum reservoir exposed there. Chemical reactions accompanying regional metamorphism, hydrothermal processes, and migration of petroleum and associated brines led to extensive mineralogical changes. These reactions, along with brittle deformation events, led to episodic changes in the hydrologic properties (i.e., porosity and permeability) of the reservoir zones within the basalt stratigraphy. The processes involved in the two most prominent chemical alteration events at Marraat, regional metamorphism and carbonate metasomatism, are discussed below along with their relationship to the temporal evolution of the petroleum system.

5.1. Regional low-grade metamorphism

Regional low-grade metamorphism of the lavas at Marraat formed a distinctive secondary mineral assemblage comprised largely of zeolites, mafic phyllosilicates, and silica phases. Such assemblages are typical of zeolite facies metamorphism of basaltic lavas, as observed throughout the rest of the North Atlantic Tertiary Igneous Province (e.g., Walker, 1960a,b; Jørgensen, 1984; Neuhoff et al., 1997, 1999, 2000) and in seafloor basalts (Alt, 1999). However, the more primitive, low-silica lava compositions dominating the Vaigat Formation exposures at Marraat led to the formation of zeolites

Table 4
Carbon and oxygen isotope values of carbonates (‰) from Marraat, West Greenland

Sample number	Morphology	$\delta^{13}C$ (PDB)	$\delta^{18}O$ (PDB)	$\delta^{18}O$ (SMOW)[a]
413403-A	Replacement	−0.89	−11.87	18.62
413403-B	Pore filling	−3.94	−16.14	14.22
413403-C	Replacement	−1.18	−10.37	20.17
413403-D	Pore filling	−3.92	−16.15	14.21
413406-A	Pore filling	3.50	−14.76	15.64
413406-B	Replacement	−2.44	−15.07	15.32
413406-C	Replacement	−5.85	−15.15	15.24
413407-B	Replacement	0.98	−15.02	15.38
413407-C	Pore filling	3.83	−13.49	16.95
413408A-A	Replacement	3.79	−16.65	13.70
413408B-A	Pore filling	5.11	−17.71	12.60
413462-A	Vein filling	−0.11	−22.01	8.17
413462-B	Vein filling	−0.57	−23.71	6.42
413462-C	Vein filling	0.08	−22.83	7.33
413464-A	Vein filling	−0.79	−21.48	8.72
413464-B	vein filling	−1.17	−22.66	7.50
447733-A	Veins w/ bitumen	3.31	−10.88	19.64
447733-B	Veins w/ bitumen	3.35	−10.73	19.80

[a] Reported values of $\delta^{18}O$ (PDB) were converted to the SMOW standard according to Hoefs (1987).

not typically observed in similar grade exposures of generally tholeiitic lavas in other areas. Specifically, the widespread occurrence of natrolite and Na-rich gonnardite, both low-Si zeolites, at Marraat contrasts with the complete absence of these phases in occurrences such as those in eastern Iceland and East Greenland (Walker, 1960b; Neuhoff et al., 1997, 1999, 2000). However, these minerals are common in the Upper and Lower Series lavas of County Antrim, Ireland (Walker, 1951, 1959, 1960a). The lavas of County Antrim are penecontemporaneous with the Vaigat Formation (Dickin, 1988) and comprise a <900 m thick section composed dominantly of picritic tholeiites that are strongly olivine-phyric (the Lower and Upper Series lavas) with more evolved tholeiitic compositions and even rhyolites present in the Middle Series (e.g., Lyle, 1985; Barrat and Nesbitt, 1996). Compositions of mafic phyllosilicates observed at Marraat are very similar to those found in the County Antrim lavas (Robert, 2001). Abundant Si-poor, Na-rich zeolites such as natrolite and gonnardite are only present in the Lower and Upper Series, and it thus appears that these assemblages likely reflect the more primitive bulk compositions of these lavas.

Estimation of the temperature and pressure conditions of regional metamorphism at Marraat is hampered by the unusual mineral assemblage developed there. Thermobarometric conditions obtained during low-grade metabasalt alteration are typically accomplished through comparison with natural analogs (e.g., Neuhoff et al., 1997, 1999, 2000) such as Icelandic geothermal systems (Kristmannsdóttir and Tómasson, 1978), fluid inclusion thermometry (e.g., Gilg et al., 2003), or Si–Al substitution thermobarometers in zeolites (Fridriksson et al., 2001; Neuhoff et al., 2004). None of these techniques is directly applicable to the assemblage at Marraat. However, inferences can be made by comparing the zeolite assemblages occurring at Marraat and County Antrim with those developed in surrounding, non-picritic lavas. Walker (1960a) mapped the depth and spatial distribution of a series of regional zeolite zones developed in the Antrim lavas. All of these mineral zones are characterized by the presence of chabazite+thomsonite, but with increasing depth analcime+natrolite and ultimately stilbite +heulandite are present. The assemblage at Marraat closely resembles that of the middle zone observed by Walker (1960a) in which analcime+natrolite are present along with chabazite and thomsonite (in the absence of stilbite and heulandite). As the estimated thickness of the succession in County Antrim is less than 1 km, even relatively high geothermal gradients (e.g., 50–60 °C/km) would result in temperatures for the natrolite- and gonnardite-bearing assemblage not exceeding ca. 80 °C. This is consistent with observations of zeolite assemblages in more evolved lavas of the Maligat Formation in West Greenland that are typically chabazite–thomsonite zone (30–70 °C; cf. Kristmannsdóttir and Tómasson, 1978) throughout the province (Neuhoff et al., 2006-this issue). Similarly low alteration temperatures (<45 °C) have been found in chabazite–phillipsite zones in basalts from the HSDP 2 drill core (Walton and Schmiffman, 2003). Hydrostatic pressures attending regional alteration

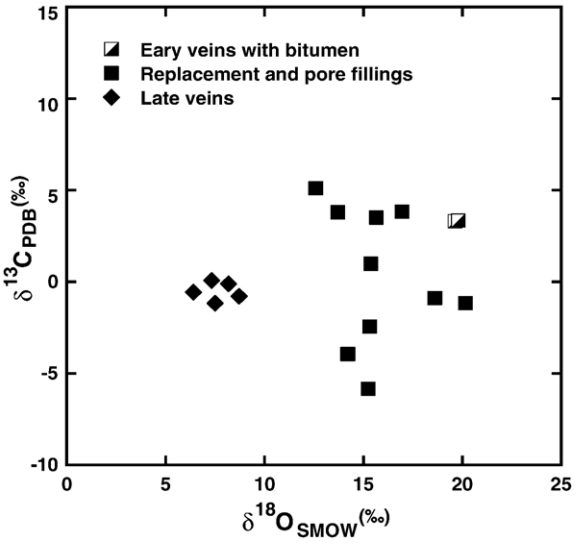

Fig. 10. The values of $\delta^{13}C_{vPDB}$ and $\delta^{18}O_{vSMOW}$ for carbonate minerals in basalts from Marraat (Table 4). Carbonates in the early veins with bitumen (half-filled squares) are dolomite ($Ca_{0.55}Mg_{0.33}Fe_{0.12}CO_3$ and $Ca_{0.51}Mg_{0.49}Fe_{0.00}CO_3$). Replacement (magnesite–siderite solid solution) and pore filling (dolomite) carbonates are represented as a group by the solid squares. Solid diamonds denote calcite in late veins (see Table 4).

at Marraat were of the order of several hundred bars, as burial depths likely did not exceed more than a few kilometers. Detailed comparisons between the alteration assemblages noted at Marraat and throughout the Vaigat Formation with those formed in feldspar-phyric lavas worldwide suggest that analcime+natrolite alteration corresponds to temperatures less than 100 °C (Neuhoff et al., 2006-this issue). In the following discussion, 70 °C is used to represent temperatures attending regional metamorphism at Marraat.

Changes in fluid composition during the formation of the regional metamorphic mineral assemblages at Marraat are interpreted with the aid of Fig. 11, which depicts the stability of the regional metamorphic mineral assemblages observed at Marraat as a function of aqueous cation to hydrogen ion activity ratios at 70 °C, and 230 bars. Small variations in temperature and pressure will affect the absolute positions of phase boundaries on these diagrams, but not the overall topology. Mineral stabilities were calculated using the program SUPCRT92 (Johnson et al., 1992) with thermodynamic data from Helgeson et al. (1978), Saccocia and Seyfried (1993), and Neuhoff (2000), and modifications compiled by E. Shock and coworkers in the slop98 database (see http://geopig.asu.edu/supcrt92/slop98.dat). End member components corresponding in stoichiometry to clinochlore and daphnite are used to represent the observed smectites and chlorites in thermodynamic calculations. Aluminum is conserved in the solid phases and the assemblages are assumed to be saturated with respect to quartz. Quartz saturation is chosen here to represent the maximum silica activity consistent with the intermittent observations of various silica polymorphs in regional alteration assemblages at Marraat.

The regional metamorphic mineral assemblage at Marraat is typical of low-grade metabasalts in that there is a clear temporal relationship between early mafic phyllosilicate formation followed by precipitation of zeolites and other Ca/Na hydrous silicates. This relationship is shown in Fig. 11A and B by the arrows representing hypothetical reaction paths corresponding to this observed mineral paragenesis. Note that the position of the reaction path in Fig. 11A lies at fluid compositions supersaturated with respect to both talc and tremolite, neither of which is observed at Marraat. However, talc can be interpreted as a component in the dioctahedral smectites that are present in this assemblage (Ransom and Helgeson, 1993). It can be seen in Fig. 11A and B that the observed mineral paragenesis, phyllosilicate formation followed by zeolites (represented by chabazite), is controlled by a decrease in the magnesium and iron activities relative to calcium activity, which has been observed in other igneous provinces in the North Atlantic (Neuhoff et al., 1999).

The most common zeolite paragenesis observed at Marraat is thomsonite followed by gonnardite, natrolite, and analcime. This zeolite paragenesis is shown as a representative reaction path on Fig. 11C, where zeolite stabilities in the Al_2O_3–SiO_2–CaO–Na_2O–H_2O system are shown as functions of cation activity ratios at 70 °C, 230 bars and quartz saturation. Gonnardite does not appear in the stability diagram due to a lack of reliable thermodynamic data, and mesolite appears in its place. This zeolite paragenesis corresponds to a decrease in the Ca/Na ratio, as well as an increase in the Si/Al ratio. This latter factor is also important in controlling the evolution of this mineral paragenesis. The absence of natrolite in Fig. 11C is due to the fact that it is stable relative to analcime only at silica activities below quartz saturation (Neuhoff, 2000).

The absence of carbonate minerals in the regional metamorphic mineral assemblages is suggestive of low CO_2 fugacities (f_{CO_2}) during regional alteration, as Ca-bearing zeolites such as thomsonite, gonnardite, and chabazite are metastable with respect to calcite-bearing assemblages at elevated f_{CO_2}. Similarly, mafic phyllosilicates are metastable with respect to assemblages containing Fe/Mg carbonates. The fluid compositions

in equilibrium with the observed regional metamorphic mineral assemblages shown in Fig. 11 can be used to evaluate the maximum possible f_{CO_2} consistent with the absence of carbonates in this assemblage (cf. Neuhoff et al., 1999). Under the conditions of Fig. 11, maximum f_{CO_2} corresponding to the absence of calcite is $10^{-5.0}$ and $10^{-5.5}$ bars, which places an upper bound on the carbon content of these fluids. Calculated values of f_{CO_2} required for destabilizing mafic phyllosilicates relative to Fe/Mg carbonates are up to four orders of magnitude higher, indicating that replacement of the regional metamorphic mineral assemblages by carbonates during petroleum migration must have been associated with significantly elevated f_{CO_2}.

5.2. Carbonate alteration at Marraat

Basalts surrounding a suite of petroleum-conducting faults in the Marraat area are altered, to varying degrees, by carbonate minerals replacing low-grade metamorphic silicates and zeolites, and filling primary porosity (vesicles and brecciated flow tops) and later vein sets. Fluid inclusion experiments on pore and vein filling carbonates at Marraat reported by Stannius (1998) indicate filling temperatures between 80 °C and 126 °C and salinities of 1.65 to 4.85 wt.% NaCl equivalent (the mode being somewhat less that seawater salinity). Although these data are limited in number, Stannius (1998) noted no difference in fluid inclusion filling temperatures or salinities

Table 5
Carbon and oxygen isotope values of calcite (‰) in basalts from West Greenland (Ubekendt island), East Greenland, and Eastern Iceland

Sample number	Location	δ^{13}C (vPDB)	δ^{18}O (vSMOW)
UB1	Ubekendt, W. Greenland	−2.1	7.6
UB2A	Ubekendt, W. Greenland	2.0	6.5
UB2B	Ubekendt, W. Greenland	2.4	7.2
UB2C	Ubekendt, W. Greenland	2.4	6.5
UB3	Ubekendt, W. Greenland	−2.0	4.1
UB4A	Ubekendt, W. Greenland	2.5	7.0
UB4B	Ubekendt, W. Greenland	−2.1	6.2
477872Vca	Ubekendt, W. Greenland	0.05	7.2
477833ca	Ubekendt, W. Greenland	−0.8	10.0
477826ca	Ubekendt, W. Greenland	2.1	6.0
UB4c	Ubekendt, W. Greenland	−1.1	5.1
UB5	Ubekendt, W. Greenland	0.2	3.9
94-41teig	Eastern Iceland	−6.9	8.14
94-99 teig	Eastern Iceland	−5.6	9.8
Ice-spar	Eastern Iceland	−3.6	7.7
Bulandsa	Eastern Iceland	−4.6	14.3
IRDP Core (185 m)	Eastern Iceland	−4.0	6.4
IRDP Core (248 m)	Eastern Iceland	−5.0	6.4
IRDP Core (277 m)	Eastern Iceland	−4.7	5.1
IRDP Core (307 m)	Eastern Iceland	−5.3	5.7
IRDP Core (308 m)	Eastern Iceland	−5.5	5.4
IRDP Core (328 m)	Eastern Iceland	−7.0	9.4
IRDP Core (583 m)	Eastern Iceland	−5.3	7.3
IRDP Core (759 m)	Eastern Iceland	−4.9	6.3
IRDP Core (921 m)	Eastern Iceland	−4.9	4.3
IRDP Core (1026 m)	Eastern Iceland	−4.8	5.0
IRDP Core (1309 m)	Eastern Iceland	−3.4	7.9
IRDP Core (1365 m)	Eastern Iceland	−4.4	4.6
IRDP Core (1390 m)	Eastern Iceland	−4.2	2.4
IRDP Core (1675 m)	Eastern Iceland	−4.6	4.3
IRDP Core (1867 m)	Eastern Iceland	−4.9	4.7
IRDP Core (1910 m)	Eastern Iceland	−5.2	5.3
EG659C-1	East Greenland	−7.3	4.7
EG659C-2	East Greenland	−8.5	4.9
EG673A	East Greenland	−13.7	7.6
EG1016F	East Greenland	−3.0	7.1
EG1061	East Greenland	−2.3	5.6
EG1225	East Greenland	−20.0	7.1
EG1237	East Greenland	−30.4	6.4
EG1237A	East Greenland	−30.9	6.8

Table 5 (*continued*)

Sample number	Location	$\delta^{13}C$ (vPDB)	$\delta^{18}O$ (vSMOW)
EG1297C	East Greenland	−14.7	6.3
EG1376	East Greenland	−4.7	6.7
EG-KF	East Greenland	1.2	5.8
426431	East Greenland	−6.2	6.3
436437	East Greenland	−26.3	7.0

Sample descriptions:
Ubekendt Island, *West Greenland*: All samples from southeast shoreline of Ubekendt Island (located ~70 km north of the Marraat area in Fig. 1). Samples are from central coarse grained sparry calcite/dolomite centers of vein systems that are ~10 s of meters wide.
Eastern Iceland: 94-41teig and 94-99teig are late stage (Stage III) pore filling calcite from the Teigarhorn region of Berufjordur (see Neuhoff et al., 1999). Ice-spar, cavity filling calcite from Iceland spar mine located near Reydarfjordur. Bulandsa, located near Beurfjordur. IRDP Core samples: disseminated or vug-filling calcite from Tertiary lavas and dykes from the Reydarfjordur drill core (Hattori and Muehlenbachs, 1982).
East Greenland: With the exception of samples EG-KF and 436437, all samples are from basalts cropping out east of the Skaergaard intrusion. EG659C-1 and -2, late stage calcite in epidote-garnet skarn, contact aureole of Miki Fjord Macrodike (see Bird et al., 1985). EG673A, southeast contact aureole of Skaergaard intrusion, epidote+quartz veins with late stage calcite+prehnite (see Bird et al., 1986; Manning and Bird, 1991). Samples EG1016, −1061, −1225, −1237, −1297 are all from the Sodalen area (see map in Nielsen et al., 1981 for details; alteration described by Bird et al., 1985, 1986; Manning and Bird, 1991, 1995). EG1016F, Canyondal, coarse grained sparry calcite filled cavity. EG1061, Sodalen Gl., late stage calcite in epidote+quartz lined cavity. EG1225, Canyondal, late stage calcite filling epidote+quartz lined cavity. EG1237 and EG1237A, Sodalen, late stage calcite filling epidote+prehnite+quartz lined cavity. EG1297C, Sodalen Gl., late stage calcite filling cavity lined with epidote +quartz followed by prehnite+quartz. EG1376, Jacobsen Fjord, late stage calcite filling cavities in prehnite mineralized dike (see Bird et al., 1985; Rose and Bird, 1994). EG-KF, calcite filling fault breccia in Kruuse Fjord layered gabbro (see Rose and Bird, 1987; Arnason et al., 1997). 426431, Nansen Fjord area, late stage calcite filled veins in epidote altered dike swarm. 436437, Urbjerget, Prinsen af Wales Bjerge, calcite in zeolite altered basalts (see Hansen et al., 2002). Note, samples EG1225, −1237, −1297, and 436437 are located in the lower most portion of the basalt stratigraphy that overlies organic-rich sediments (see Nielsen et al., 1981).

among the various vein or primary pore filling carbonates. The fluid inclusion observations suggest that aqueous solutions associated with carbonate alteration were only slightly warmer (~10–50 °C) than those attending regional metamorphism. Slightly elevated temperatures may be expected due to combined effects of (*i*) upward migration along fault zones of warmer fluids from deep in the sedimentary section, and (*ii*) local heat input related to dikes and sills (Karup-Møller, 1969; Binzer and Karup-Moller, 1974; Christiansen et al., 1996). Nonetheless, temperatures were not sufficiently high to cause large-scale thermal destabilization of the preexisting mineral assemblages or petroleum.

While carbonates filling veins at Marraat are dominantly calcite and dolomite, carbonates found within the primary pore space replacing preexisting secondary

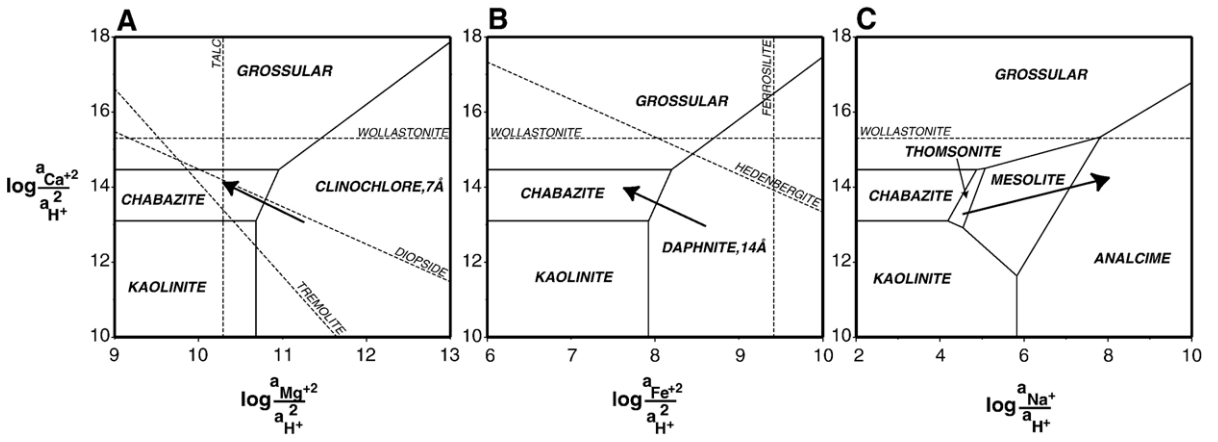

Fig. 11. Mineral stabilities at 70 °C and 230 bars are depicted as a function of cation activity ratios in the Al_2O_3–Na_2O–CaO–MgO–FeO–SiO_2–H_2O–HCl system. The activity diagrams were calculated using SUPCRT92 (Johnson et al., 1992) and thermodynamic data from Helgeson et al. (1978), Neuhoff (2000), Saccocia and Seyfried (1993), and the slop98 database (see text) assuming Al balance, quartz saturation and $a(H_2O)=1$. The dashed lines indicate saturation surfaces of the minerals indicated. Analcime is replaced by natrolite at low aqueous silica activities. Thomsonite and mesolite are considered in place of gonnardite due to the lack of reliable thermodynamic data for this phase. The arrows represent hypothetical reaction paths based on observed mineral parageneses.

silicates and filling residual pore space typically include more Fe, Mg-rich compositions along the magnesite–siderite join. Relative timing relations among various generations of carbonates within the primary pore spaces suggest a general paragenetic sequence of magnesite–siderite followed by dolomite and ultimately calcite. This trend, and the generally more Mg, Fe-rich compositions of the replacement and pore filling carbonates relative to the vein carbonates suggests that much of the Mg and Fe was sourced from the regionally-metamorphosed basalts themselves. In fact, the paragenetic sequence mimics the trend of increasing Ca/Mg and Ca/Fe ratios observed during regional metamorphism of these basalts (see above) and other low-grade metabasalts (i.e., Neuhoff et

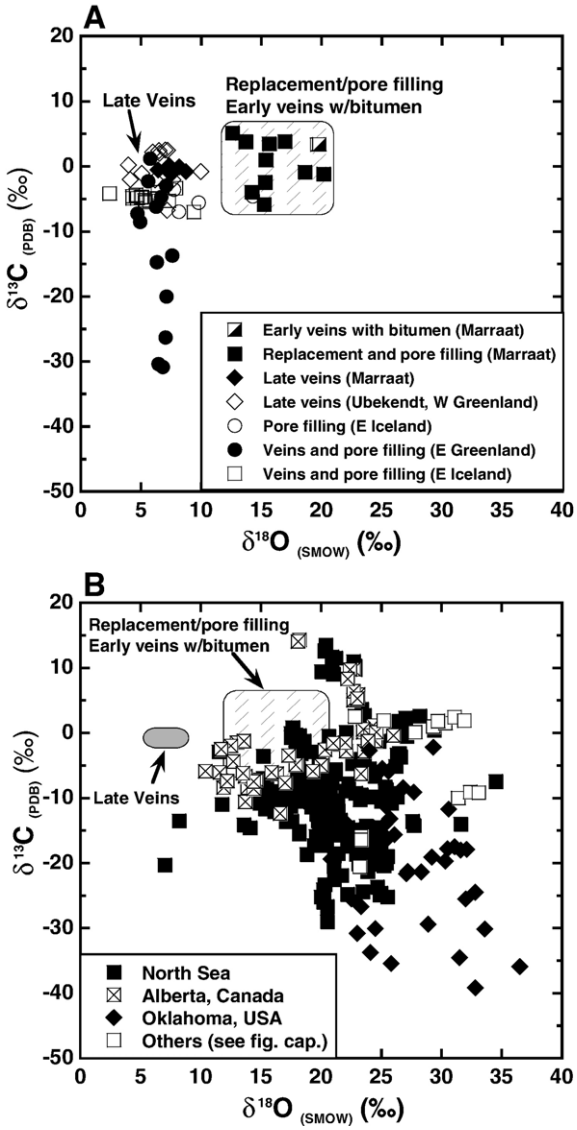

Fig. 12. The values of $\delta^{13}C_{vPDB}$ and $\delta^{18}O_{vSMOW}$ for carbonates in basalts from Marraat (Table 4) and for carbonate minerals in (A) basalts from Ubekendt Island (West Greenland), Eastern Iceland (open squares — Iceland research drill hole), and East Greenland (Table 5), and in (B) sediment hosted petroleum reservoirs worldwide. The hatched rectangle in A and B denotes the range of values for early bitumen veins and replacement and pore filling carbonates at Marraat; the solid diamonds in A and the oval shaded area in B denote values for calcite in the late veins at Marraat. In diagram B, data for carbonates from petroleum reservoirs in the North Sea are from Emery et al. (1993), Kantorowicz (1985), Macaulay et al. (1993), McLaughlin et al. (1994), Stewart et al. (2000), and Walderhaug and Bjorkum (1992); data for carbonates from petroleum reservoirs in Alberta, Canada are from Ayalon and Longstaffe (1988), Dimitrakopoulos and Muehlenbachs (1987), and Longstaffe and Ayalon (1987); values for carbonates associated with petroleum microseepage at Cement, Oklahoma, are from Donovan (1974); symbols marked "Others" denotes carbonates in petroleum reservoirs from Brazil, Malagasy, Zaire, California, Indonesia, Sicily, and Alberta are from Table II of Dimitrakopoulos and Muehlenbachs (1987).

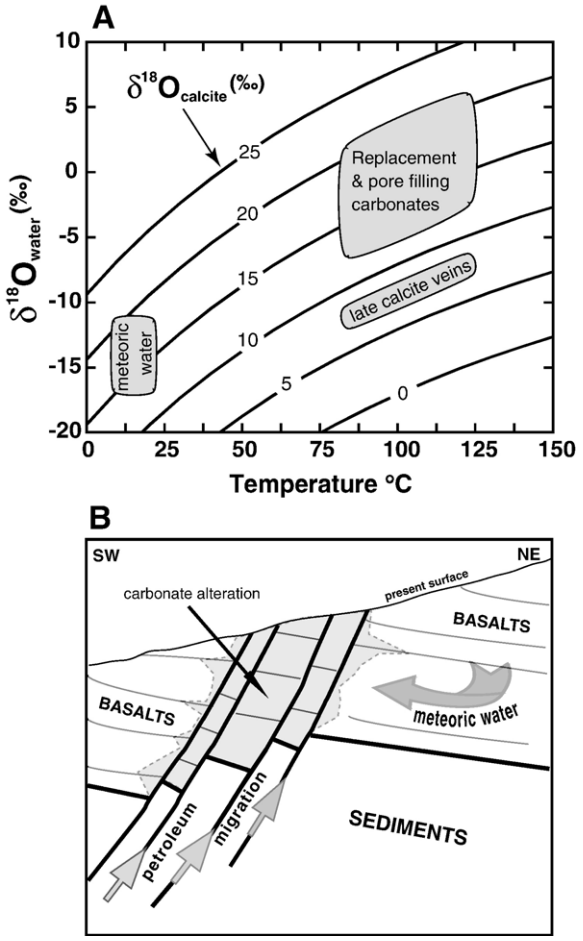

Fig. 13. Oxygen isotope and hydrologic interpretation of fluids responsible for carbonate alteration at Marraat. (A) Temperature dependence of $\delta^{18}O_{vSMOW}$ in water in equilibrium with calcite calculated from equations and data reported by O'Neil et al. (1969), showing predicted range for early Tertiary "meteoric water" (see text for details), and $\delta^{18}O_{vSMOW}$ in carbonates (Table 4) for *i*) replacement, pore filling and bitumen containing veins, and *ii*) late stage calcite veins over the range of temperatures reported by Stannius (1998; 80–126 °C). (B) Schematic southwest to northeast cross-section of the Marraat area, showing hypothetical fluid flow paths from the underlying sedimentary basin and circulation of meteoric water in the overlying basalts (see text for details).

al., 1999). Dissolution of preexisting secondary minerals and perhaps unaltered portions of the basalts accessed by veins led to the initially elevated Mg and Fe contents of the carbonate mineralizing fluids. This was critical for the widespread migration of CO_2-rich fluids into the basalts that likely had very low porosities and permeabilities after regional metamorphism. While multiple carbonate vein sets are recognized at Marraat, the isotopic evidence below suggests that widespread infiltration and alteration of the lavas by the carbonate mineralizing fluids did not attend all of the vein events.

Values of $\delta^{13}C_{vPDB}$ and $\delta^{18}O_{vSMOW}$ of carbonates at Marraat form two distinct populations (Fig. 10): (1) paragenetically early dolomite veins and magnesite–siderite replacement of low-grade metamorphic minerals that have $\delta^{18}O_{vSMOW}$ between 12.6 and 20‰ and $\delta^{13}C_{vPDB}$ in the approximate range of 0 ± 5‰, and (2) late stage calcite veins that are lighter in ^{18}O ($\delta^{18}O_{vSMOW}$ between 6.4 and 8.7‰) and have a restricted range of $\delta^{13}C_{vPDB}$ values that are near zero. In general, as carbonate alteration progresses, values of $\delta^{18}O_{vSMOW}$ decrease and values of $\delta^{13}C_{vPDB}$ approach zero. To evaluate the origin of fluids responsible for carbonate alteration of the basalts we employ comparative analysis of the Marraat data (Table 4) with carbon and oxygen isotope data of carbonate minerals from basalts elsewhere in West Greenland and in the North Atlantic Igneous Province (Table 5 and Fig. 12A), and with carbonate minerals formed in sediment hosted petroleum reservoirs worldwide (Fig. 12B).

There is a notable similarity in the range of $\delta^{18}O_{vSMOW}$ between late-stage calcite veins at Marraat and carbonates in basalts from West Greenland, East Greenland, and

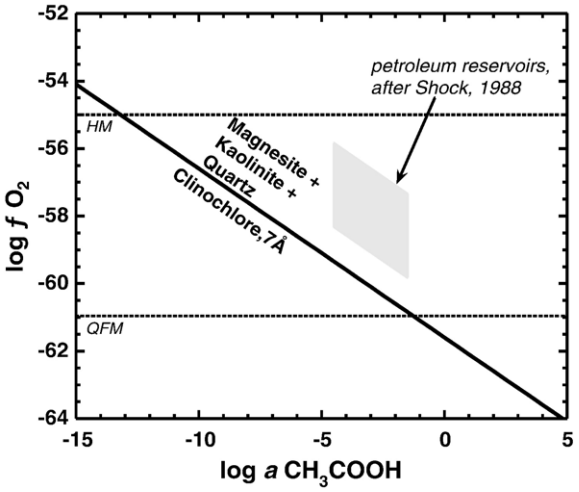

Fig. 14. The stability of clinochlore relative to carbonates is shown as a function of log f_{O_2} and the log activity of acetic acid at 100 °C and 300 bars. The solid line indicates equilibrium for reaction (4). The values of log f_{O2} for the hematite–magnetite (HM) and fayalite–magnetite–quartz (FMQ) mineral buffers are shown as dashed horizontal lines. The shaded area indicates typical oil field brine conditions (see text for details) after Shock, 1988, 1989, 1994. Calculations made using SUPCRT92 (Johnson et al., 1992) and thermodynamic data from Helgeson et al. (1978), Saccocia and Seyfried (1993), and the slop98 data base (see text).

Iceland (Fig. 12A). Because Tertiary hydrothermal/metamorphic fluids within basalts of East Greenland and in eastern Iceland were primarily of meteoric origin (Taylor and Forester, 1978; Hattori and Muehlenbachs, 1982; Fehlhaber and Bird, 1991; Kristmanssdóttir and Sveinbjörnnsdóttir, 1992; Nevle et al., 1994), it seems likely that meteoric water was a major component in fluids forming late-stage calcite veins at Marraat, as well as the late-stage coarse grained carbonate vein centers analyzed from Ubekendt Island (open diamonds Fig. 12A). Similar correlation of $\delta^{13}C_{vPDB}$ between late-stage calcites from Marraat and calcites from Iceland and the majority of the East Greenland samples again points to the role of meteoric fluids, which is supported by the narrow range of $\delta^{13}C_{vPDB}$ near 0‰, indicative of equilibration with atmospheric carbon dioxide. Carbonates from East Greenland with values of $\delta^{13}C_{vPDB}$ less than −10‰ are, with the exception of sample 673A, all from the lower most basalts overlying organic-rich sediments (see sample descriptions in Table 5). Such low values of $\delta^{13}C_{vPDB}$ are likely due to oxidative decomposition of organic compounds (cf. Longstaffe, 1987, 1989; Macaulay et al., 2000).

The range of oxygen and carbon isotope properties of carbonates from Marraat (Table 4) are shown in Fig. 12B where they can be compared with analyses from 327 carbonates formed within petroleum reservoirs in the North Sea (Kantorowicz, 1985; Walderhaug and Bjorkum, 1992; Emery et al., 1993; Macaulay et al., 1993; McLaughlin et al., 1994; Stewart et al., 2000), Alberta, Canada (Dimitrakopoulos and Muehlenbachs, 1987; Longstaffe and Ayalon, 1987; Ayalon and Longstaffe, 1988), Oklahoma, USA (Donovan, 1974), and petroleum reservoirs in Brazil, Malagasy, Zaire, California, Indonesia, Sicily, and Alberta (marked as "Others" in Fig. 12B; Dimitrakopoulos and Muehlenbachs, 1987). In general, there is a close correlation among the range of carbonates formed by replacement, pore filling and veins with bitumen at Marraat (hatched area in Fig. 12B) and the range of analyses for carbonates from petroleum reservoirs worldwide. The latter are characterized by: (1) high values of $\delta^{18}O_{vSMOW}$ that result from varying mixtures of basinal/petroleum brines and meteoric water that have reacted with sedimentary rocks, and (2) a wide range in $\delta^{13}C_{vPDB}$ resulting from decomposition of migrating petroleum in the presence of water, with oxidative biodegradation resulting in carbonates with negative values of $\delta^{13}C_{vPDB}$, and anoxic bacterial fermentation resulting in carbonates with positive $^{13}C_{vPDB}$ values (Gould and Smith, 1978; Dimitrakopoulos and Muehlenbachs, 1987; Longstaffe, 1987, 1989; Macaulay et al., 1993, 1998, 2000; Stewart et al., 2000).

We summarize our geologic, paragenetic and isotopic observations of carbonate mineralization at Marraat in Fig. 13. Diagram A of this figure shows the temperature dependence of $\delta^{18}O_{vSMOW}$ for water in equilibrium with calcite calculated from equations and data reported by O'Neil et al. (1969). We use oxygen isotope fractionation between calcite and water as a proxy for the carbonates at Marraat. For comparative analysis the area marked "meteoric water" in the diagram denotes the range of δ^{18} O_{vSMOW} for central East Greenland meteoric water

between ~55 to 40 Ma, computed from values of δD_{water} reported by Nevle et al. (1994) and equations and data reported by Rozanski et al. (1993). The shaded areas in Fig. 13A are the range in fluid inclusion temperatures (80–126 °C, Stannius, 1998) and $\delta^{18}O_{vSMOW}$ in carbonates (Table 4) for (1) replacement, pore filling and bitumen containing veins, and (2) late stage calcite veins. Replacement magnesite–siderite, and pore and vein filling dolomite associated with petroleum migration are formed from waters with $\delta^{18}O_{vSMOW}$ between ~ −6 and +6‰, and are interpreted as varying mixtures of basinal brines, meteoric water, and petroleum migrating up faults from the Late Cretaceous–Early Paleocene sediments to the overlying basalts. This fluid flow path is represented by the three upward pointing arrows in the schematic cross-section of Fig. 13B. In contrast, fluids in equilibrium with the late calcite veins have $\delta^{18}O_{vSMOW}$ values that are in the range of −13 to −7‰ (Fig. 13A). These fluids are interpreted to be primarily of meteoric origin that have reacted to varying degrees with the basalt stratigraphy, and to have a fluid flow path schematically represented by the curved arrow in Fig. 13B.

The replacement of regional metamorphic mineral assemblages by carbonate and quartz assemblages associated with petroleum migration required significant modifications of the porosity and permeability structure of the basalt stratigraphy. Regional metamorphism significantly reduced of porosity by infilling primary pore space with zeolites and mafic phyllosilicates. Textural changes in the basalt matrix associated with replacement of primary phases by secondary minerals also contributed to a significant reduction in permeability. The abundant carbonate vein sets at Marraat are clear evidence of an increase in porosity and permeability associated with brittle deformation that permitted migration of CO_2-rich fluids into the lavas. However, carbonate replacement textures within vesicular zones surrounding fractures and faults indicate that either there was *i*) still sufficient permeability for the carbonate mineralizing fluids to penetrate the lavas after regional metamorphism, or *ii*) that secondary porosity and permeability was generated by the fluids themselves as preexisting phases dissolved in the carbonate-rich fluids. The pervasiveness of silicate mineral destabilization relative to carbonate-bearing assemblages suggest that the latter phenomenon likely played a large role in determining the hydrologic properties of the volcanic aquifer during carbonate metasomatism and ultimately provided sufficient storage capacity for trapping reservoir-scale petroleum accumulations observed at Marraat.

An interesting feature of the mineralization at Marraat is that carbonate minerals within the lavas are restricted to replacements and infilling of amygdules. Although the matrix of the lavas between vesicles is altered to mineral assemblages similar in both mineralogy and phase composition as observed in the vesicles, the matrix is largely unaffected by carbonate mineralization. The cause of this phenomenon is unclear but may reflect preferential migration of CO_2-bearing fluids through the vesicular zones along the same flow paths that were active during regional metamorphism. Regardless of the cause, this observation may have important implications for the capacity of basaltic lavas to serve as long-term storage reservoirs for CO_2. It suggests that the volume of carbonate minerals that will form within basalt is controlled in part by the primary porosity.

Although carbonate mineralization appears restricted to primary pore space, the amount of CO_2 fixed in the crust during the alteration events at Marraat is significant. For instance, if all of the carbonate mineralization is in the form of dolomite (which has a molar volume of 184.4 cm^3/mol, intermediate between those of magnesite and calcite), then a vesicular zone within a lava that contains 20% vesicles by volume could potentially fix ~2170 mol CO_2 per m^3 of lava. On a regional scale, if one assumes that the bulk primary porosity of the lavas is ca. 5% (accounting for massive flow interiors that make up a large proportion of individual lava flows) and a volume of altered lavas of 300 km^3 (a conservative estimate based on the exposed outcrop area of metasomatized lavas on Nuussuaq), then carbonate metasomatism within this province may have sequestered $\sim 2\times10^{14}$ mol CO_2. This value corresponds to ~0.3% of the total CO_2 in the Earth's atmosphere (6.2×10^{16} mol; Sleep and Zahnle, 2001).

The observations detailed above may be of considerable consequence for the geological storage of carbon dioxide (cf. Klara et al., 2003; Baines and Worden, 2004; Johnson et al., 2004; Rochelle et al., 2004). First, the observation that carbonate mineralization is restricted to pore space (including previously occluded pore space) may be an important consideration for selecting injection sites within basaltic lava sequences. Second, it is clear that despite the low volumetric percentage of a lava flow that is affected by carbonate mineralization, large masses of CO_2 can be fixed through carbonate alteration of basalts. However, it remains unclear how injection of supercritical CO_2 would differ from the events that took place at Marraat both in terms of transport processes and reactivity.

5.3. Redox conditions within basalt-hosted petroleum reservoirs

High concentrations of organic acids (up to 10,000 mg/L) are found in oil-field brines at temperatures

ranging from 25 to 200 °C (Dickey et al., 1972; Carothers and Kharaka, 1978; Lundegard, 1985; Workman and Hanor, 1985; Hanor and Workman, 1986; Kharaka et al., 1986, 1987; Barth, 1987; Fisher, 1987; Means and Hubbard, 1987; Land et al., 1988; MacGowan and Surdam, 1988; Connolly et al., 1990; Fisher and Boles, 1990; Modavanyi, 1990; Barth, 1991; Abercrombie, 1991; Land and Macpherson, 1992a,b). Helgeson et al. (1993) showed that aqueous organic acids in oil-field brines are products of the irreversible hydrolytic disproportionation of short-chain ($n \leq \sim 6$–9) alkanes in petroleum at the oil–water interface. Acetic and propanoic acids, and their anions, consistently dominate the aqueous organic carbon species in oil-field brines (Kharaka et al., 1993a,b, 2000). Furthermore, Shock (1988) showed that measurements of acetic acid worldwide correspond to aqueous activities between $10^{-4.5}$ and $10^{-1.5}$. While there are no measurements of aqueous organic acids in the fluids at Marraat, we assume that they are present at Marraat and at concentrations similar to those observed elsewhere in oil field brines.

Organic acids in oil-field brines have been shown to affect secondary mineral stability in sedimentary petroleum reservoirs by affecting the pH and f_{CO_2} (Crossey et al., 1984; Franks and Forester, 1984; Gautier and Claypool, 1984; Surdam et al., 1984; Gautier, 1986; Shock, 1988, 1989; Fisher and Boles, 1990; MacGowan and Surdam, 1990; Helgeson et al., 1993; Bennett and Casey, 1994; Giles et al., 1994; Pittman and Hathon, 1994; Shock, 1994; Surdam and Yin, 1994). In addition, organic acids appear to control the oxidation state of the oil-field brines. For example, Shock (1988, 1989, 1994) determined that aqueous organic acids in oil-field brines maintain metastable redox equilibrium with CO_2 and with each other according to

$$\underset{\text{(acetic acid)}}{CH_3COOH} + 2O_2 \leftrightarrow 2CO_2 + 2H_2O \quad (1)$$

and

$$\underset{\text{(propanoic acid)}}{2CH_3CH_2COOH} + O_2 \leftrightarrow 3\underset{\text{(acetic acid)}}{CH_3COOH}. \quad (2)$$

Helgeson et al. (1993) proposed that the reduced carbon in petroleum and oxidized carbon in carbonate approach metastable redox equilibrium through the production of aqueous organic compounds. While the sources of CO_2 and aqueous organic acids are not necessarily the same (Shock, 1997), migration of petroleum and brine increases the total aqueous carbon concentrations, including both CO_2 and acetic acid. Thus, aqueous organic acids may buffer the fugacities of oxygen and carbon dioxide and ultimately control secondary mineral stability and diagenetic reactions in petroleum reservoirs. Most observations of redox equilibria between acetic acid and CO_2 have been in sedimentary reservoirs in which the bulk rock has little potential of controlling the redox state of the system. In contrast, redox-sensitive mineral assemblages (i.e., olivine, pyroxene and magnetite) are abundant in basalt-hosted petroleum reservoirs. Thus they provide an important test of the relative importance of mineral versus fluid compositional controls on oxidation state in petroleum reservoirs and the concomitant effects on mineral paragenesis and petroleum stability.

Coupled equilibrium between organic acid-bearing fluids and secondary mineral assemblages observed at Marraat can be evaluated by combining reaction (1) with reactions describing replacement of zeolites and mafic phyllosilicates by carbonate minerals. For example, in the system $CaO–MgO–Al_2O_3–SiO_2–H_2O–CO_2$ the reaction describing replacement of the clinochlore component in mafic phyllosilicate solid solutions by the magnesite component in the magnesite–siderite solid solutions and quartz can be described by the reaction,

$$\underset{\text{(clinochlore)}}{Mg_5Al_2Si_3O_{10}(OH)_8} + 5CO_{2(g)} \leftrightarrow \underset{\text{(kaolinite)}}{Al_2Si_2O_5(OH)_4} + 5\underset{\text{(magnesite)}}{MgCO_3} + \underset{\text{(quartz)}}{SiO_2} + 2H_2O, \quad (3)$$

where kaolinite, although not observed at Marraat, is included as a constraint on the maximum Al content of the resulting fluids. Reactions (1) and (3) are combined to give,

$$\underset{\text{(clinochlore)}}{Mg_5Al_2Si_3O_{10}(OH)_8} + 2.5\underset{\text{(acetic acid)}}{CH_3COOH} + 5O_2 \leftrightarrow \underset{\text{(kaolinite)}}{Al_2Si_2O_5(OH)_4} + 5\underset{\text{(magnesite)}}{MgCO_3} + \underset{\text{(quartz)}}{SiO_2} + 7H_2O, \quad (4)$$

for which the equilibrium constant is,

$$\log K_{(4)} = 5 \log a_{\text{magnesite}} - 5 \log f_{O_2} - 2.5 \log a_{\text{acetic acid}} - \log a_{\text{clinochlore}}, \quad (5)$$

where a denotes the activities of aqueous and mineral species, taken to be unity for quartz, kaolinite and water,

and f_{O_2} denotes the fugacity of oxygen. Provided activities of the mineral end member components of mafic phyllosilicates and carbonates can be assessed, Eq. (5) allows the stability of the mineral assemblages of reaction (4) to be assessed as a function of f_{O_2} and $a_{\text{acetic acid}}$. The solid line in Fig. 14 depicts the stability of clinochlore relative to magnesite+quartz+kaolinite as a function of these variables at 100 °C and 300 bars (conditions consistent with the observations detailed above for the carbonate replacement reactions). This phase boundary was calculated assuming stoichiometric clinochlore and magnesite (i.e., unit activities for these phases) as it is presently impossible to evaluate with certainty the activity of the clinochlore end member in the mafic phyllosilicate compositions observed at Marraat. However, the effect of solid solution in mafic phyllosilicates and magnesite–siderite solid solutions will tend to cancel each other out as these phases appear on opposite sides of reaction (4). The fugacity of CO_2 for equilibrium of reaction (4) is about 10^{-1} bars. The shaded area in Fig. 14 defines the entire range of measured acetic acid concentrations and the range of f_{O_2} possible over a range of f_{CO_2} from 1 bar to total pressure at metastable equilibrium (after Shock, 1988, 1989, 1994). The shaded area therefore represents the conditions typical of oil-field brines and those inferred to have been associated with petroleum migration at Marraat.

Inspection of Fig. 14 shows that the replacement of mafic phyllosilicates by carbonates is favored under conditions typical of oil-field brines. Fluid compositions typical of oil field brines (shaded box) lie within the stability field of the magnesite-bearing assemblage in reaction (4) indicating that mafic phyllosilicates would react with such fluids to form Mg-rich carbonates and silica. No Al-containing phases are observed in the carbonate mineral parageneses at Marraat, suggesting that Al is mobile during the process, either due to complexation by organic acids or as a result of the low pH values associated with the elevated organic acid and carbonate contents of the fluids. Similar calculations for replacement of daphnite (the Fe analog of clinochlore) by siderite and Ca-zeolites by calcite are also consistent with this result (cf. Neuhoff et al., 2000; Rogers, 2000). Also shown in Fig. 14 is f_{O_2} consistent with equilibria for the hematite+magnetite (HM) and fayalite+magnetite+quartz (FMQ) mineral assemblages. The latter assemblage is likely a good approximation of the initial oxidation state of the olivine- and spinel-rich picritic basalts at Marraat. It can be seen that at conditions associated with the FMQ assemblage, replacement of clinochlore by magnesite is only possible at acetic acid concentrations in excess of those observed in any active petroleum system (e.g., Dickey et al., 1972; Carothers and Kharaka, 1978; Lundegard, 1985; Workman and Hanor, 1985; Hanor and Workman, 1986; Kharaka et al., 1986, 1987; Fisher, 1987; Means and Hubbard, 1987; Barth, 1987; Land et al., 1988; MacGowan and Surdam, 1988; Connolly et al., 1990; Fisher and Boles, 1990; Modavanyi, 1990; Barth, 1991; Abercrombie, 1991; Land and Macpherson, 1992a, b). A similar relationship is found for zeolite–carbonate equilibria at FMQ conditions (Neuhoff et al., 2000; Rogers, 2000). Thus it appears that the oxidation state of the fluids associated with petroleum migration and carbonate mineralization at Marraat was controlled not by the basalt mineralogy, but rather by the compositions of the fluids themselves as has been suggested in sedimentary reservoirs.

6. Concluding remarks

Basalt-hosted petroleum reservoirs are unique geochemical environments where complex interactions among aqueous solutions, basalts and hydrocarbons can affect mineral stability and fluid flow properties. The subaerial exposures at Marraat provide a unique opportunity to study the chemical and physical processes occurring in these systems. Although observations in other basalt-hosted petroleum reservoirs are limited (Hoshi, 1988; Pendkar and Kumar, 1999), extensive CO_2 metasomatism and carbonate mineralization associated with petroleum migration appears to be one common aspect of these systems, and one that may well be important in determining the quality of reservoir properties in basalts.

In addition, the extent of carbonate alteration at Marraat may represent an important natural analog for carbon sequestration in basaltic lavas. The pervasiveness of carbonate alteration, even away from the carbonate vein sets, attests to the relative ease of infiltration of carbonate-bearing fluids into even extensively altered low-grade metabasalts. These observations hold promise for attempts at sequestering carbon dioxide in carbonate minerals in such systems.

Acknowledgements

Field work was conducted by two of us (P.S.N and A. K.P.) as part of a field expedition organized by F.G. Christiansen and funded by the Geological survey of Denmark and Greenland (GEUS), who also provided additional support for this study. Support was also provided by the U.S. Environmental Protection Agency (graduate fellowship to PSN), National Science Foundation (NSF-EAR 95-06469 and 0001113 to DKB; graduate fellowship to KLR), Stanford University

(graduate fellowship to KLR) and Washington University Olin Fund (graduate fellowship to KLR). L. Stannius and A. Boesen assisted with the fieldwork and B. Jones and T. Horten assisted with analytical work. L. Gonzalez and S. Carpenter provided stable isotopic analyses of carbonates performed at The University of Iowa. This work benefited from helpful discussions with F.G. Christensen, J. Boejesen-Koefoed, L.M. Larsen, G.K. Pedersen, M. Schulte, and Th. Fridriksson. We'd like to thank Jeffrey Alt and Peter Schiffman for their thoughtful reviews and Stefan Bernstein for the editorial handling of this manuscript. This paper is published with the permission from the Geological Survey of Denmark and Greenland.

References

Abercrombie, H.J., 1991. Reservoir processes in steam-assisted recovery of bitumen, Leming pilot, Cold Lake, Alberta, Canada: compositions, mixing, and sources of co-produced waters. Applied Geochemistry 6, 495–508.

Alt, J.C., 1999. Very low-grade hydrothermal metamorphism of basic igneous rocks. In: Frey, M., Robinson, D. (Eds.), Low-Grade Metamorphism. Blackwell Science, Oxford, pp. 169–201.

Arnason, J.G., Bird, D.K., Bernstein, S., Rose, N.M., Manning, C.E., 1997. Petrology and geochemistry of the Kruuse Fjord gabbro complex, East Greenland. Geological Magazine 134, 67–89.

Arnórsson, S., Gunnarsson, I., Stefansson, A., Andresdóttir, A., Sveinbjörnnsdóttir, A.E., 2002. Major element chemistry of surface- and ground waters in basaltic terrain, N-Iceland. I. Primary mineral saturation. Geochimica et Cosmochimica Acta 66, 4015–4046.

Ayalon, A., Longstaffe, F.J., 1988. Oxygen isotope studies of diagenesis and pore-water evolution in the western Canada sedimentary basin: evidence from the Upper Cretaceous basal Belly River sandstone, Alberta. Journal of Sedimentary Petrology 58, 489–505.

Baines, S.J., Worden, R.H., 2004. The long-term fate of CO_2 in the subsurface: natural analogues for CO_2 storage. In: Baines, S.J., Worden, R.H. (Eds.), Geological Storage of Carbon Dioxide. The Geological Society of London, London, pp. 59–86.

Barrat, J.A., Nesbitt, R.W., 1996. Geochemistry of the Tertiary volcanism of Northern Ireland. Chemical Geology 129, 15–38.

Barth, T., 1987. Quantitative determination of volatile carboxylic acids in formation waters by isotachophoresis. Analytical Chemistry 59, 2232–2237.

Barth, T., 1991. Organic acids and inorganic ions in waters from petroleum reservoirs, Norwegian continental shelf: a multivariate statistical analysis and comparison with American reservoir formation waters. Applied Geochemistry 6, 1–15.

Bennett, P.C., Casey, W., 1994. Chemistry and mechanisms of low-temperature dissolution of silicates by organic acids. In: Pittman, E.D., Lewan, M.D. (Eds.), Organic Acids in Geological Processes. Springer-Verlag, Berlin, pp. 162–200.

Binzer, K., Karup-Moller, S., 1974. Ferri-sepiolite in hydrothermal calcite–quartz–chalcedony veins in Nugssuaq in West Greenland. Meddelelser om Grønland 114, 15.

Bird, D.K., Rosing, M.T., Manning, C.E., Rose, N.M., 1985. Geologic field studies of the Miki Fjord area, East Greenland. Meddelelser fra Dansk Geologisk Forening 34, 219–236.

Bird, D.K., Rogers, D., Manning, C.E., 1986. Mineralized fracture systems of the Skaergaard intrusion, East Greenland. Meddelelser om Grønland 16, 1–68.

Bojesen-Koefoed, J., Christiansen, F.G., Nytoft, H.P., Dalhoff, F., 1997a. Organic Geochemistry and Thermal Maturity of Sediments in the GRO#3 Well, Nuusuaq, West Greenland. 97/43. Danmarks og Grønlands Geologiske Undersøgelse.

Bojesen-Koefoed, J., Christiansen, F.G., Nytoft, H.P., Pedersen, A.K., 1997b. Seep data from onshore West Greenland. 97/34. Danmarks og Grønlands Geologiske Undersøgelse.

Bojesen-Koefoed, J.A., Christiansen, F.G., Nytoft, H.P., Pedersen, A. K., 1999. Oil seepage onshore West Greenland: evidence of multiple source rocks and oil mixing. In: Fleet, A.J., Boldy, S.A. R. (Eds.), Petroleum Geology of Northwest Europe: Proceedings of the 5th Conference. Geological Society of London, London, pp. 305–314.

Carothers, W.W., Kharaka, Y.K., 1978. Aliphatic acid anions in oil-field waters — implications for origin of natural gas. AAPG Bulletin 62, 2441–2453.

Chalmers, J.A., Pulvertaft, T.C.R., 2001. Development of the continental margins of the Labrador Sea: a review. In: Wilson, R.C.L., Whitmarsh, R.B., Taylor, B., Froitzheim, N. (Eds.), Non-Volcanic Rifting of Continental Margins: a Comparison of Evidence from Land and Sea. The Geological Society of London, London, pp. 77–105.

Chalmers, J.A., Pulvertaft, T.C.R., Marcussen, C., Pedersen, A.K., 1999. New insight into the structure of the Nuussuaq Basin, central West Greenland. Marine and Petroleum Geology 16, 197–224.

Christiansen, F.G., 1993. Disko Bugt Project 1992, West Greenland. Rapp. Grønlands Geologiske Undersøgelse, vol. 159, pp. 47–52.

Christiansen, F.G., 1994. Seeps and other Bitumen Showings: A Review of the Origin, Nomenclature and Occurrences in Greenland. 94/7. Grønlands Geologiske Undersøgelse.

Christiansen, F.G., Dam, G., Pedersen, A.K., 1994. Discovery of live oil at Marraat, Nuussuaq: field work, drilling and logging. Rapport Grønlands Geologiske Undersøgelse 160, 60–65.

Christiansen, F.G., Bojesen-Koefoed, J., Dam, G., Nytoft, H.-P., Larsen, L.M., Pedersen, A.K., Pulvertaft, T.C.R., 1996. The Marraat oil discovery on Nuussuaq, West Greenland: evidence for a latest Cretaceous–earliest Tertiary oil prone source rock in the Labrador Sea–Melville Bay region. Bulletin of Canadian Petroleum Geology 44 (1), 39–54.

Christiansen, F.G., Boesen, A., Bojesen-Koefoed, J.A., Dalhoff, F., Dam, G., Neuhoff, P.S., Pedersen, A.K., Pedersen, G.K., Stannius, L.S., Zinck-Joergensen, K., 1998. Petroleum geological activities onshore West Greenland in 1997. Geology of Greenland Survey Bulletin 180, 10–17.

Christiansen, F.G., Boesen, A., Bojesen-Koefoed, J., Chalmers, J.A., Dallhoff, F., Dam, G., Hjortkjaer, B.F., Kristensen, L., Larsen, L.M., Marcussen, C., Mathiesen, A., Nohr-Hansen, H., Pedersen, A.K., Pedersen, G.K., Pulvertaft, T.C.R., Skaarup, N., Sonderholm, M., 1999. Petroleum geological activities onshore West Greenland in 1998. Geology of Greenland Survey Bulletin 183, 46–56.

Clarke, D.B., Pedersen, A.K., 1976. Tertiary volcanic province of West Greenland. In: Escher, A., Watt, W.S. (Eds.), Geology of Greenland. Geological Survey of Greenland, Copenhagen, Denmark, pp. 364–385.

Connolly, C.A., Walter, L.M., Baadsgaard, H., Longstaffe, F.J., 1990. Origin and evolution of formation waters, Alberta Basin, western Canada sedimentary basin. I. Chemistry. Applied Geochemistry 5, 375–395.

Crossey, L.J., Frost, B.R., Surdam, R.C., 1984. Secondary porosity in laumontite-bearing sandstones. In: McDonald, D.A., Surdam, R.C.

(Eds.), Clastic Diagenesis. The American Association of Petroleum Geologists, Tulsa, pp. 225–238.

Dam, G., 2002. Sedimentology of magmatically and structurally controlled outburst valleys along rifted volcanic margins; examples from the Nuussuaq Basin, West Greenland. Sedimentology 49, 505–532.

Dam, G., Sonderholm, M., 1994. Lowstand slope channels of the Itilli succession (Maastrichtian–Lower Paleocene), Nuussuaq, West Greenland. Sedimentary Geology 94, 49–71.

Dickey, P.A., Collins, A.G., Fajardo, M.I., 1972. Chemical composition of deep formation waters in southwestern Louisiana. AAPG Bulletin 56, 1530–1570.

Dickin, A.P., 1988. The North Atlantic Tertiary Province. In: MacDougal, J.D. (Ed.), Continental Flood Basalts. Kluwer, Dordrecht, The Netherlands, pp. 111–149.

Dimitrakopoulos, R., Muehlenbachs, K., 1987. Biodegradation of petroleum as a source of ^{13}C-enriched carbon dioxide in the formation of carbonate cement. Chemical Geology 65, 283–291.

Donovan, T.J., 1974. Petroleum microseepage at Cement, Oklahoma: evidence and mechanism. AAPG Bulletin 58, 429–446.

Emery, D., Smalley, P.C., Oxtoby, N.H., 1993. Synchronous oil migration and cementation in sandstone reservoirs demonstrated by quantitative description diagenesis. Philosophical Transactions of the Royal Society of London 344, 115–125.

Fehlhaber, K.L., Bird, D.K., 1991. Oxygen-isotope exchange and mineral alteration in gabbros of the Lower Layered Series, Kap Edvard Holm Complex, East Greenland. Geology 19, 819–822.

Fisher, J.B., 1987. Distribution and occurrence of aliphatic acid anions in deep subsurface waters. Geochimica et Cosmochimica Acta 51, 2459–2468.

Fisher, J.B., Boles, J.R., 1990. Water–rock interaction in Tertiary sandstones, San Joaquin basin, California, U.S.A.: diagenetic controls on water composition. Chemical Geology 82, 83–101.

Franks, S.G., Forester, R.W., 1984. Relationships among secondary porosity, pore-fluid chemistry and carbon dioxide, Texas Gulf Coast. In: McDonald, D.A., Surdam, R.C. (Eds.), Clastic Diagenesis. The American Association of Petroleum Geologists, Tulsa, pp. 63–80.

Freeze, R.A., Cherry, J.A., 1979. Groundwater. Prentice-Hall Inc., New Jersey.

Fridriksson, T., Neuhoff, P.S., Arnorsson, S., Bird, D.K., 2001. Geologic constraints on the thermodynamic properties of stilbite–stellerite solid solutions in low-grade metabasalts. Geochimica et Cosmochimica Acta 65, 3993–4008.

Gautier, D.L. (Ed.), 1986. Roles of Organic Matter in Sediment Diagenesis. Society of Economic Paleontologists and Mineralogists Special Publication, vol. 38. Society of Economic Paleontologists and Mineralogists, Tulsa, OK. 203 pp.

Gautier, D.L., Claypool, G.E., 1984. Interpretation of methanic diagenesis in ancient sediments by analogy with processes in modern diagenetic environments. In: McDonald, D.A., Surdam, R.C. (Eds.), Clastic Diagenesis. The American Association of Petroleum Geologists, Tulsa, pp. 111–123.

Giles, M.R., Boer, R.B.D., Marshall, J.D., 1994. How important are organic acids in generating secondary porosity in the subsurface? In: Pittman, E.D., Lewan, M.D. (Eds.), Organic Acids in Geological Processes. Springer-Verlag, Berlin, pp. 449–470.

Gilg, H.A., Morteani, G., Kostisyn, Y., Preinfalk, C., Gatter, I., Streider, A.J., 2003. Genesis of amethyst geodes in basaltic rocks of the Serra Geral Formation (Ametista do Sul, Rio Grande do Sul, Brazil): a fluid inclusion, REE, oxygen, carbon, and Sr isotope study on basalt, quartz, and calcite. Mineralalium Deposita 38, 1009–1025.

Gould, K.W., Smith, J.W., 1978. Isotopic evidence for microbiological role in genesis of crude oil from Barrow Island, Western Australia. AAPG Bulletin 62, 455–462.

Hald, N., Pedersen, A.K., 1975. Lithostratigraphy of the early Tertiary volcanic rocks of central West Greenland. Grønlands Geologiske Undersøgelse 69, 17–24.

Hanor, J.S., Workman, A.L., 1986. Distribution of dissolved volatile fatty acids in some Louisiana oil field brines. Applied Geochemistry 1, 37–46.

Hansen, H., Pedersen, A.K., Duncan, R.A., Bird, D.K., Brooks, C.K., Fawcett, J.J., Gittins, J., Gorton, M., O'Day, P., 2002. Volcanic stratigraphy of the southern Prinsen af Wales Bjerge region, East Greenland. In: Jolley, D.W., Bell, B.R. (Eds.), The North Atlantic Igneous Province: Stratigraphy, Tectonics, Volcanic and Magmatic Processes. The Geological Society of London, London, pp. 183–218.

Hattori, K., Muehlenbachs, K., 1982. Oxygen isotope ratios of the Icelandic crust. Journal of Geophysical Research 87 (B8), 6559–6565.

Helgeson, H.C., Delany, J.M., Nesbitt, H.W., Bird, D.K., 1978. Summary and critique of the thermodynamic properties of rock-forming minerals. American Journal of Science 278-A, 1–229.

Helgeson, H.C., Knox, A.M., Owens, C.E., Shock, E.L., 1993. Petroleum, oil field waters, and authigenic mineral assemblages: are they in metastable equilibrium in hydrocarbon reservoirs? Geochimica et Cosmochimica Acta 57, 3295–3339.

Henderson, G., 1969. Oil and gas prospects in the Cretaceous–Tertiary basin of West Greenland. Grønlands Geologiske Undersøgelse 22, 23.

Henderson, G., 1975. Stratigraphy and structure of the Tertiary volcanic rocks of the Marrait Kitdlit area, Nuqssuaq. Grønlands Geologiske Undersøgelse 69, 11–16.

Henderson, G., Schiener, E.J., Risum, J.B., Croxton, C.A., Andersen, B.B., 1981. The West Greenland basin. In: Kerr, J.W. (Ed.), Geology of the North Atlantic Borderlands, Memoir. Canadian Society of Petroleum Geology, pp. 399–428.

Hoefs, J., 1987. Stable Isotope Geochemistry. Springer-Verlag, Berlin. 241 pp.

Hoshi, K., 1988. Miocene ocean floor metamorphism during back-arc spreading in the Japan Sea. Ph.D. Thesis, Stanford University.

Johnson, J.W., Oelkers, E.H., Helgeson, H.C., 1992. SUPCRT92: a software package for calculating the standard molal thermodynamic properties of minerals, gases, aqueous species, and reactions among them as functions of temperature and pressure. Computers & Geosciences 18, 899–947.

Johnson, J.W., Nitao, J.J., Knauss, K.G., 2004. Reactive transport modeling of CO_2 storage in saline aquifers to elucidate fundamental processes, trapping mechanism and sequestration partitioning. In: Baines, S.J., Worden, R.H. (Eds.), Geological Storage of Carbon Dioxide. The Geological Society of London, pp. 107–128.

Jørgensen, O., 1984. Zeolite zones in the basaltic lavas of the Faeroe Islands. Annales Societatia Scientarium Faroensis, Supplementum 9, 71–91.

Kantorowicz, J.D., 1985. The origin of authigenic ankerite from the Ninian field, UK North Sea. Nature 315, 214–216.

Karup-Møller, S., 1969. Xonotlite-, pectolite- and natrolite-bearing fracture veins in volcanic rocks form Nuussuaq, West Greenland. Grønlands Geologiske Undersøgelse 80, 4–20.

Kharaka, Y.K., Law, L.M., Carothers, W.W., Goerlitz, D.F., 1986. Role of organic species dissolved in formation waters from sedimentary basins in minerals diagenesis. In: Gautier, D.L. (Ed.), Roles of Organic Matter in Sediment Diagenesis. Society of Economic Paleontologists and Mineralogists Special Publication, vol. 38. Society of Economic Paleontologists and Mineralogists, Tulsa, OK, pp. 111–122.

Kharaka, Y.K., Maest, A.S., Carothers, W.W., Law, L.M., Lamothe, P.J., Fries, T.L., 1987. Geochemistry of metal-rich brines from central Mississippi salt dome basin, USA. Applied Geochemistry 2, 543–561.

Kharaka, Y.K., Ambats, G., Thorsden, J.J., 1993a. Distribution and significance of dicarboxylic acid anions in oil field waters. Chemical Geology 107, 499–501.

Kharaka, Y.K., Lundegard, P.D., Ambats, G., Evans, W.C., Bischoff, J.L., 1993b. Generation of aliphatic acid anions and carbon dioxide by hydrous pyrolysis of crude oils. Applied Geochemistry 8, 317–324.

Kharaka, Y.K., Lundegard, P.D., Giordano, T.H. (Eds.), 2000. Distribution and origin of organic ligands in subsurface waters from sedimentary basins. Ore genesis and exploration: the roles of organic matter. Reviews in Economic Geology, vol. 9, pp. 119–131.

Klara, S.M., Srivastava, R.D., McIlvried, H.G., 2003. Integrated collaborative technology development program for CO_2 sequestration in geologic formations — United States Department of Energy R & D. Energy Conversion and Management 44, 2699–2712.

Kristmannsdóttir, H., Tómasson, J., 1978. Zeolite zones in geothermal areas in Iceland. In: Sand, L.B., Mumpton, F.A. (Eds.), Natural Zeolites. Pergamon Press, Oxford, UK, pp. 277–284.

Kristmanssdóttir, H., Sveinbjörnnsdóttir, A.E., 1992. Changes of stable isotopes and chemistry of fluids in the low-temperature geothermal field at Bakki-Thoroddstadir, Olfus, SW-Iceland. In: Kharaka, Y., Maest, A.S. (Eds.), Water–Rock Interaction. Balkema, Rotterdam, pp. 951–954.

Land, L.S., Macpherson, G.L., Mack, L.E., 1988. The geochemistry of saline formation waters, Miocene, offshore Louisiana. Transactions — Gulf Coast Association of Geological Societies 38, 503–511.

Land, L.S., Macpherson, G.L., 1992a. Geothermometry from brine analyses: lessons from the Gulf Coast, USA. Applied Geochemistry 7, 333–340.

Land, L.S., Macpherson, G.L., 1992b. Origin of saline formation waters, Cenozoic section, Gulf of Mexico sedimentary basin. AAPG Bulletin 76, 1344–1362.

Longstaffe, F.G., 1987. Stable isotope studies of diagenetic processes. In: Kyser, T.K. (Ed.), Stable Isotope Geochemistry of Low Temperature Fluids. Mineralogical Association of Canada Short Course, Toronto, pp. 187–257.

Longstaffe, F.J., 1989. Stable isotopes as tracers in clastic diagenesis. In: Hutcheon, I.E. (Ed.), Burial Diagenesis. Mineralogical Society of Canada, pp. 210–277.

Longstaffe, F.J., Ayalon, A., 1987. Oxygen isotope studies of clastic diagenesis in the lower Cretaceous Viking formation, Alberta: implication for the role of meteoric water. In: Marshall, J.D. (Ed.), Diagenesis of Sedimentary Sequences. Geological Society Special Publication. Geological Society of London, Oxford, pp. 277–296.

Lundegard, P.D., 1985. Carbon Dioxide and Organic Acids: Origin and Role in Burial Diagenesis (Texas Gulf Coast Tertiary). University of Texas, Austin, TX.

Lyle, P., 1985. The petrogenesis of the Tertiary basaltic and intermediate lavas of Northeast Ireland. Scottish Journal of Geology 21, 71–84.

Macaulay, C.I., Haszeldine, R.S., Fallick, A.E., 1993. Distribution, chemistry, isotopic composition and origin of diagenetic carbonates: Magnus Sandstone, North Sea. Journal of Sedimentary Petrology 63, 33–43.

Macaulay, C.I., Fallick, A.E., Haszeldine, R.S., Pearson, M.J., 1998. The significance of $\delta^{13}C$ of carbonate cements in reservoir sandstone: a region perspective from the Jurassic of the northern North Sea. In: Morad, S. (Ed.), Carbonate Cementation in Sandstones: Distribution Patterns and Geochemical Evolution. Blackwell, Oxford, pp. 395–408.

Macaulay, C.I., Fallick, A.E., Haszeldine, R.S., Macauley, G.E., 2000. Oil migration makes the difference: regional distribution of carbonate cement $\delta^{13}C$ in northern North Sea Tertiary sandstones. Clay Minerals 35, 69–76.

MacGowan, D.B., Surdam, R.C., 1988. Difunctional carboxylic acid anions in oilfield waters. Organic Geochemistry 12, 245–259.

MacGowan, D.B., Surdam, R.C., 1990. Carboxylic acid anions in formation waters, San Joaquin Basin and Louisiana Gulf Coast, U. S.A.— implications for clastic diagenesis. Applied Geochemistry 5, 687–701.

Manning, C.E., Bird, D.K., 1991. Porosity evolution and fluid flow in the basalts of the Skaergaard magma–hydrothermal system, East Greenland. American Journal of Science 291, 201–257.

Manning, C.E., Bird, D.K., 1995. Porosity, permeability, and basalt metamorphism. In: Schiffman, P., Day, H.W. (Eds.), Low-Grade Metamorphism of Mafic Rocks. Geological Society of America, Boulder, CO, pp. 123–140.

McLaughlin, O.M., Haszeldine, R.S., Fallick, A.E., Rogers, G., 1994. The case of the missing clay: aluminum loss and secondary porosity, South Brae Oilfield, North Sea. Clay Minerals 29, 1651–1663.

Means, J.L., Hubbard, N., 1987. Short-chain aliphatic acid anions in deep subsurface brines: a review of their origin, occurrence, properties, and importance and new data on their distribution and geochemical implications in the Palo Duro Basin, Texas. Organic Geochemistry 11, 177–191.

Metcalf, R., Banks, D., Bottrell, S.H., 1992. An association between organic matter and localized, prehnite–pumpellyite alteration, at Builth Wells, Wales, U.K. Chemical Geology 102, 1–21.

Modavanyi, E.P., 1990. Evolution of basinal brines: elemental and isotopic evolution of formation waters and diagenetic minerals during burial of carbonate sediments, Upper Jurassic Smackover Formation, southwest Arkansas, US Gulf Coast, Washington University, St. Louis.

Neuhoff, P.S., 2000. Thermodynamic properties and parageneses of rock-forming zeolites. Ph.D. Thesis, Stanford University, Stanford, CA, 240 pp.

Neuhoff, P.S., Bird, D.K., 1994. Theoretical analysis of laumontite stability in the presence of organic acid rich fluids. Geological Society of American Abstracts with Programs 26 (7), A-278.

Neuhoff, P.S., Watt, W.S., Bird, D.K., Pedersen, A.K., 1997. Timing and structural relations of regional zeolite zones in basalts of the East Greenland continental margin. Geology 25, 803–806.

Neuhoff, P.S., Fridriksson, T., Arnorsson, S., Bird, D.K., 1999. Porosity evolution and mineral paragenesis during low-grade metamorphism of basaltic lavas at Teigarhorn, Eastern Iceland. American Journal of Science 299, 467–501.

Neuhoff, P.S., Fridriksson, T., Bird, D.K., 2000. Zeolite parageneses in the North Atlantic Igneous Province: implications for geotectonics and groundwater quality of basaltic crust. International Geology Review 42, 15–44.

Neuhoff, P.S., Hovis, G.L., Balassone, G., Stebbins, J.F., 2004. Thermodynamic properties of analcime solid solutions. American Journal of Science 304, 21–66.

Neuhoff, P.S., Stannius, L.S., Rogers, K.L., Bird, D.K., Pedersen, A.K., 2006-this issue. Regional zeolite-facies metamorphism of basaltic lavas. Disko-Nuussuaq region, West Greenland Lithos 92, 33–54. doi:10.1016/j.lithos.2006.03.028.

Nevle, R.J., Brandriss, M.E., Bird, D.K., McWilliams, M.O., O'Neil, J.R., 1994. Tertiary plutons monitor climate change in East Greenland. Geology 22, 775–778.

Nielsen, T.F.D., Soper, N.J., Brooks, C.K., Fuller, A.M., Higgins, A.C., Matthews, D.W., 1981. The pre-basaltic sediments and the lower basalts at Kangordlugssuaq, East Greenland: their stratigraphy, lithology, paleomagnetism and petrology. Meddelelser om Grønland 6, 1–25.

O'Neil, J.R., Clayton, R.N., Mayeda, T.K., 1969. Oxygen isotope fractionation in divalent metal carbonates. Journal of Chemical Physics 51, 5547–5558.

Pedersen, A.K., 1985. Lithostratigraphy of the Tertiary Vaigat Formation on Disko, central West Greenland. Grønlands Geologiske Undersøgelse 124, 1–30.

Pedersen, A.K., 1986. Indication of migrated hydrocarbons in Tertiary volcanic rocks from western Nuussuaq, central West Greenland. Grønlands Geologiske Undersøgelse 130, 32–35.

Pedersen, A.K., Pulvertaft, T.C.R., 1992. The nonmarine Cretaceous of the West Greenland Basin, onshore West Greenland. Cretaceous Research 13, 263–272.

Pedersen, A.K., Larsen, L.M., Riisager, P., Dueholm, K.S., 2002. Rates of volcanic deposition, facies changes and movements in a dynamic basin: the Nuussuaq Basin, West Greenland, around the C27n–C26r transition. In: Jolley, D.W., Bell, B.R. (Eds.), The North Atlantic Igneous Province: Stratigraphy, Tectonics, Volcanic, and Magmatic Processes. The Geological Society of London, London, pp. 157–181.

Pendkar, N., Kumar, 1999. Delineation of reservoir section in Deccan Trap basement, example from Padra Field, Cambay Basin. Proc. Workshop on Integrated Exploration for Stratigraphic and Subtle Traps, Dehradun. Bulletin of the Oil and Natural Gas Corporation Limited 36, 83–88.

Pittman, E.D., Hathon, L.A., 1994. Material balance considerations for the generation of secondary porosity by organic acids and carbonic acid derived from kerogen, Denver Basin, Colorado, USA. In: Pittman, E.D., Lewan, M.D. (Eds.), Organic Acids in Geological Processes. Springer-Verlag, Berlin, pp. 115–137.

Ransom, B., Helgeson, H.C., 1993. Compositional end members and thermodynamic components of illite and dioctahedral aluminous smectite solid solutions. Clays and Clay Minerals 41 (5), 537–550.

Robert, C., 2001. Hydrothermal alteration processes in the Tertiary lavas of Northern Ireland. Mineralogical Magazine 65, 543–554.

Rochelle, C., Czernichowski-Lauriol, I., Milodowski, A.E., 2004. The impact of chemical reactions on CO_2 storage in geological formations: a brief review. In: Baines, S.J., Worden, R.H. (Eds.), Geological Storage of Carbon Dioxide. The Geological Society of London, London, pp. 87–106.

Rogers, K.L., 2000. Mineral paragenesis and CO_2 metasomatism in a basalt-hosted petroleum reservoir, Nuussuaq, West Greenland. M.S. Thesis, Stanford University, 115 pp.

Rose, N.M., Bird, D.K., 1987. Prehnite–epidote phase relations in the Nordre Aputiteq and Kruusen Fjord layered gabbros, East Greenland. Journal of Petrology 28, 1193–1218.

Rose, N.M., Bird, D.K., 1994. Hydrothermally altered dolerite dikes in East Greenland: implication for Ca-metasomatism of basaltic protolith. Contributions to Mineralogy and Petrology 116, 420–432.

Rozanski, K., Araguas-Araguas, L., Gonfiantini, R., 1993. Isotopic patterns in modern global precipitation. In: Swart, P.K., Lohmann, K.C., McKenzie, J., Savin, S. (Eds.), Climate Change in Continental Isotopic Records. American Geophysical Union, Washington, DC, pp. 1–36.

Saccocia, P.J., Seyfried, J.W.E., 1993. A resolution of discrepant thermodynamic properties for chamosite retrieved from experimental and empirical techniques. American Mineralogist 78, 607–611.

Shock, E.L., 1988. Organic acid metastability in sedimentary basins. Geology 16, 886–890.

Shock, E.L., 1989. Corrections to "Organic acid metastability in sedimentary basins". Geology 17, 572–573.

Shock, E.L., 1994. Application of thermodynamic calculations to geochemical processes involving organic acids. In: Pittman, E.D., Lewan, M.D. (Eds.), Organic Acids in Geological Processes. Springer-Verlag, Berlin, pp. 270–318.

Shock, E.L. (Ed.), 1997. Thermodynamic response of organic compounds in geochemical processes in sedimentary basins. Ore genesis and exploration: the roles of organic matter. Reviews in Economic Geology, vol. 9, pp. 105–117.

Sleep, N.H., Zahnle, K., 2001. Carbon dioxide cycling and implication for climate on ancient earth. Journal of Geophysical Research 106, 1373–1399.

Stannius, L.S., 1998. Hydrothermal alteration, zeolite formation, and oil impregnation of basalts in the Marraat area, Nuussuaq, West Greenland. M.Sc. Thesis, University of Copenhagen, Copenhagen, Denmark.

Stefansson, A., Gislason, S.R., 2001. Chemical weathering of basalts, southwest Iceland: effect of rock crystallinity and secondary minerals on chemical fluxes to the ocean. American Journal of Science 301, 513–556.

Stewart, R.N.T., Haszeldine, R.S., Fallick, A.E., Wilkinson, M., Macaulay, C.I., 2000. Regional distribution of diagenetic carbonate cement in Palaeocene deepwater sandstones: North Sea. Clay Minerals 35, 119–133.

Storey, M., Duncan, R.A., Pedersen, A.K., Larsen, L.M., Larsen, H. C., 1998. $^{40}Ar/^{39}Ar$ geochronology of the West Greenland Tertiary volcanic province. Earth and Planetary Science Letters 160, 569–586.

Surdam, R.C., Yin, P., 1994. Organic acids and carbonate stability, the key to predicting positive porosity anomalies. In: Pittman, E.D., Lewan, M.D. (Eds.), Organic Acids in Geological Processes. Sringer, Verlag, Berlin, pp. 398–448.

Surdam, R.C., Boese, S.W., Crossey, L.J., 1984. The chemistry of secondary porosity. In: McDonald, D.A., Surdam, R.C. (Eds.), Clastic Diagenesis. The American Association of Petroleum Geologists, Tulsa, pp. 127–150.

Taylor, H.P., Forester, R.W., 1978. Oxygen and hydrogen isotope evidence for the origin, development and circulation pattern of the meteoric–hydrothermal convective system associated with the 50-m.y. old Skaergaard basaltic magma chamber, East Greenland. Geological Society of American Abstracts with Programs 10, 503.

Tingle, T.N., Neuhoff, P.S., Ostergren, J.D., Jones, R.E., Donovan, J.J., 1996. The effect of 'missing' (unanalyzed) oxygen on quantitative electron microprobe microanalysis of hydrous silicate and oxide minerals. Geological Society of American Abstracts with Programs 28, A-212.

Walderhaug, O., Bjorkum, P.A., 1992. Effect of meteoric water flow on calcite cementation in the middle Jurassic Oseburg formation, well 30/3-2, Veslifrikk Field, Norwegian North Sea. Marine and Petroleum Geology 9, 308–318.

Walker, G.P.L., 1951. The amygdale minerals in the Tertiary lavas of Ireland. I. The distribution of chabazite habits and zeolites in the Garron Plateau area, County Antrim. Mineralogical Magazine 29, 773–791.

Walker, G.P.L., 1959. The amygdale minerals in the Tertiary lavas of Ireland. II. The distribution of gmelinite. Mineralogical Magazine 32, 202–217.

Walker, G.P.L., 1960a. The amygdale minerals in Tertiary lavas of Ireland. III. Regional distribution. Mineralogical Magazine 32, 773–791.

Walker, G.P.L., 1960b. Zeolite zones and dike distribution in relation to the structure of the basalts in eastern Iceland. Journal of Geology 68, 515–528.

Walton, A.W., Schmiffman, P., 2003. Alteration of hyaloclastites in the HSDP 2 Phase 1 drill core. 1. Description and paragenesis. Geochemistry, Geophysics, Geosystems 4 (5) (31 pp.).

Workman, A.L., Hanor, J.S., 1985. Evidence for large-scale vertical migration of dissolved fatty acids in Louisiana oil field brines: Iberia Field, south-central Louisiana. Transactions — Gulf Coast Association of Geological Societies 35, 293–300.